

Transport and Kinetics at Carbon Nanotube –Redox Enzyme Composite Modified Electrode Biosensors

Part 2. Redox enzyme dispersed in nanotube mesh of finite thickness

Michael E G Lyons *

Physical and Materials Electrochemistry Laboratory, School of Chemistry, University of Dublin, Trinity College, Dublin 2, Ireland

*E-mail: melyons@tcd.ie

Received: 31 August 2009 / Accepted: 15 September 2009 / Published: 30 September 2009

A mathematical model describing the transport and kinetics of substrate and redox mediator in surface deposited films of finite thickness is described. These bio-catalytically active chemically modified electrodes comprise redox enzymes immobilized in a highly dispersed mesh of single walled carbon nanotubes (SWNT) which are in turn immobilized on a support metal surface. A small molecule redox mediator is used to both regenerate the reduced enzyme and to transfer electrons either to the carbon nanotube surface or to the underlying support electrode surface thereby generating a current which can be measured. The pertinent transport and kinetic differential equations of both substrate and redox mediator are formulated along with suitable boundary conditions and are solved analytically to derive suitable approximate analytical expressions for the current response expected for the system under steady state batch amperometric conditions. The kinetics of substrate and mediator within the nanotube layer are summarized in terms of a kinetic case diagram.

Keywords: Amperometric enzyme biosensor modeling; SWNT modified electrodes; enzyme bioelectrocatalysis ; immobilized redox enzyme systems

1. INTRODUCTION

In a recent feature article Li, Wang and Chen [1] described nano-bioelectrochemistry as a new interdisciplinary field which provides scope for much exciting development, innovation and new discovery over the next few years. This emerging field combines interfacial electrochemistry, biochemistry and biocatalysis and nanoscience and has as a central aim the full understanding and use of biological electron transfer processes in well defined nanostructured environments which can be

used as platforms for emerging biosensor and bioelectronic applications and devices. This area has been recently reviewed by a number of authors [2-11]. In a recent review by Willner and Katz [6] it was stated that 'integration of redox enzymes with an electrode support and formation of an electrical contact between the biocatalyst and the electrode is the fundamental object of bioelectronics and optobioelectronics'. More generally the nanoscale will define the region where the physical and engineering science of the 21st century will be pursued, elaborated and utilized [12-15]. Since their discovery by Iijima [16] in 1993, carbon nanotubes (both multiwalled and single walled, designated MWNT and SWNT respectively) have attracted enormous international interest because of their perceived unique structural, mechanical and electronic properties [17-22]. In addition the redox and catalytic properties of electrodes modified with both MWNT and SWNT have recently been examined [23-36]. These types of nano-heterogeneous systems have been typical exemplifiers of chemically modified electrodes which have been extensively studied for over 30 years [37-43].

A key concept associated with chemically modified electrodes is that of redox mediation. In this process surface immobilized sites may be activated electrochemically via application of a potential to the support electrode. The latter sites may then oxidize or reduce other redox agents located in the solution phase adjacent to the immobilized layer, for which the direct oxidation or reduction at the electrode surface is inhibited, either because of intrinsically slow heterogeneous electron transfer kinetics, or because close approach of the soluble redox species to the electrode is prevented. The idea is presented schematically in figure 1 where the processes of direct unmediated electron transfer and mediated electron transfer at an electrode are compared.

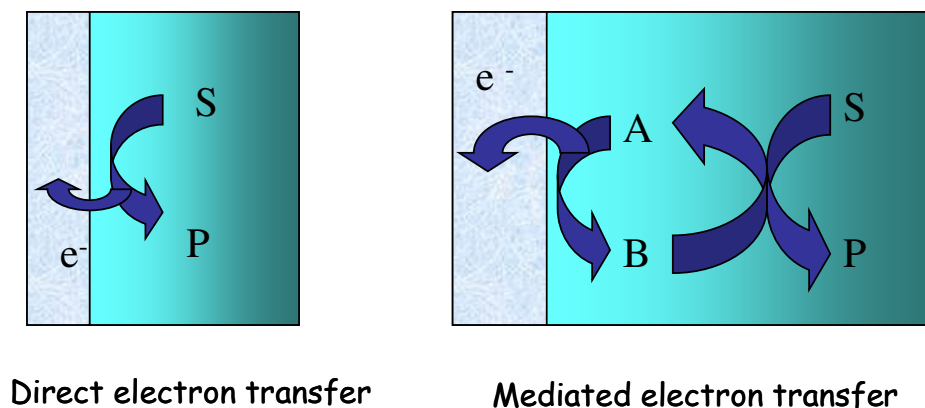


Figure 1. Schematic representation of direct and mediated electron transfer at the electrode/solution interface.

Of course the attractive feature of chemically modified electrodes lies in the fact that the deposited chemical microstructure or bio-recognition element can be the subject of bottom up rational design and be tailormade to perform a specific task. The 'bottom up' construction of nano-structured assemblies using catalytic enzymes, small molecule redox mediators and immobilized matrices can be challenging, and the successful combination of all three components to form a successfully operating biocatalytic system necessitates a detailed understanding of the fundamental kinetic and transport processes which may occur within the surface immobilized nanostructure. This is best accomplished

by developing a mathematical model which captures the essential physics and chemistry which encompass the key happenings in the process of biosensor operation namely, the transport of reactant (often called analyte or substrate) to the surface immobilized biorecognition element, and the chemical reaction dynamics between the substrate and the latter. It is usually assumed that the substrate transport mechanism can be ascribed to diffusion (transport in a concentration gradient). The rate law governing the interaction between substrate and biocatalyst can then be specified. Hence the modeling procedure involves problem formulation in terms of specifying a particular differential equation which involves diffusion and chemical reaction components. This reaction-diffusion (RD) equation may in general be time dependent and the chemical term may well be of a form such that the net RD equation is non-linear. It is solved subject to specific initial and boundary conditions to obtain an expression for the reaction flux or equivalently, the current flow and hence the amperometric response in terms of pertinent experimentally measurable parameters such as substrate and mediator concentration, enzyme loading, layer thickness and so on. The mathematical solution may sometimes be analytical, or more often, numerical. This type of analysis has been described for a variety of model systems [44-61]. Early theoretical work on transport and kinetics in immobilized enzyme biosensor systems has been reported by Albery and co-workers [62-64], Bartlett et al [65-70] and others [71]. More recently comprehensive theoretical papers by Saveant and co-workers [72-77], Lyons [78-82], Kulys and Baronas [83] and by Gooding et al [84-87] have been published.

Electron transfer in biological systems is one of the leading areas in the biochemical and biophysical sciences [88-90] and in recent years there has been considerable interest in the direct electron transfer between redox proteins and electrode surfaces [91-98]. However in the absence of mobile mediating small molecules, the observation of well defined electrochemical behaviour of immobilized flavoprotein oxidase systems such as glucose oxidase (GOx) is rendered extremely difficult, because the active FAD group is embedded deep within the protein structure thereby making the transmission coefficient for direct electron transfer between the latter and the support electrode very small [99,100]. Various immobilization strategies [101,102] have been adopted to fabricate enzyme electrodes for biosensor applications. These strategies have exhibited variable degrees of success and in many cases electron transfer mediators have been used to facilitate electronic communication between the active site of the protein and the underlying electrode. However the potential at which an amperometric enzyme biosensor is operated depends on the redox potential of the mediator used rather than that exhibited by the active site of the redox enzyme. Usually the difference in magnitude between the latter potentials is significant (typically ca. 0.3 - 0.5V) and is a factor which acts against successful biosensor operation, since the more positive the operating potential, the greater is the tendency for the sensor to respond to oxidizable substances present in their sample other than the target substrate. Clearly the best strategy for successful enzyme biosensor fabrication is to devise a configuration by which electrons can directly transfer from the redox center of the enzyme to the underlying support electrode. This has been accomplished in recent years using the concept of molecular wiring.

The similarity in length scales between carbon nanotubes and redox enzymes suggest the presence of interactions that may be favourable for biosensor application [9,23]. The strategy of physical adsorption or covalent immobilization of large biomolecules onto the surface of immobilized

carbon nanotubes may well represent an exciting pathway through which direct electrical communication between support electrodes and the active site of redox enzymes can be achieved. For instance recent work [103-107] has indicated that the chemical modification of electrode surfaces with carbon nanotubes has enhanced the activity of the latter with respect to the reaction of biologically active species such as hydrogen peroxide, dopamine and NADH. Furthermore multi-walled carbon nanotubes have been shown to exhibit good electronic communication with redox proteins where not only the redox center is close to the proteins surface such as found with cytochrome c, azurin and horseradish peroxidase, but also when it is embedded deep with the glycoprotein sheath such as is found with glucose oxidase [29, 108- 111].

In a recent communication describing amperometric glucose detection at SWNT mesh modified glassy carbon and gold electrodes incorporating dispersed immobilized glucose oxidase, Lyons and Keeley [110] have reported that catalytic activity with respect to glucose oxidation is observed only when a soluble mediator such as oxygen or ferrocene monocarboxylic acid is present in the solution. Catalytic glucose oxidation does not occur if adsorbed glucose oxidase is only present. The homogeneous mediator is required to ensure efficient charge shuttling between the flavin active site buried deep within the protein sheath and the underlying carbon nanotube sidewall. It was suggested that mediator molecules such as oxygen or ferrocene monocarboxylic acid molecules are of the correct size to enter the glycoprotein sheath effectively and interact with the flavin group. It is important to note that the carbon nanotube and the enzyme molecule share a similar length scale and so the enzyme is able to adsorb on the nanotube sidewall without losing its biologically active shape, form and function. Indeed Baughman and co-workers [103] have suggested the striking analogy of piercing a balloon with a long sharp needle such that the balloon does not burst. Instead by a gentle twisting action the needle can be made to enter the balloon without catastrophe. Similarly it was proposed by Lyons and Keeley [110] that some number of nanotubes are able to pierce the glycoprotein shell of glucose oxidase and gain access to the flavin prosthetic group such that the electron tunnelling distance is minimized and consequently electron transfer probability optimized. Such access is not generally afforded with traditional smooth electrodes.

In the present paper we further develop a theoretical model which describes transport and kinetics at electrodes which have been chemically modified with highly dispersed meshes of single wall carbon nanotubes on which redox enzymes such as glucose oxidase have been adsorbed. The first paper in this series [112] examined the transport and kinetics within a very thin film of SWNT in which the bio-catalytic enzyme had been immobilized. In the present paper we develop this idea and examine substrate and redox mediator transport and kinetics within a SWNT film of finite thickness L in which a redox enzyme such as glucose oxidase has been homogeneously dispersed. Two cases of practical interest will be examined. The first pertains when the nanotube strands are electrically conducting. The second applies when the strands are not so conducting and the redox mediator is regenerated at the underlying support electrode surface. In a subsequent paper [113] we will describe the somewhat more complex situation where metal nanoparticle decorated SWNT strands are used and the redox mediator can be regenerated along the length of the nanotube strands. In this more complex situation the balance between macroscopic linear diffusion throughout the film and microscopic spherical diffusion to the catalytic nanoparticle must be considered [44, 114-116].

The analysis presented in the present paper will extend and further develop theoretical ideas proposed by Bartlett and Whittaker [66], Bartlett and Pratt [68], Lyons and co-workers [47] and by Albery et al [64]. The latter papers focused on developing an approximate analytical description of finite diffusion coupled with non-linear Michaelis-Menten kinetics involving redox enzymes immobilized within electronically conducting polymer matrices. In the present work the analysis is extended to chemically modified electrode surfaces in which the redox enzyme molecules are homogeneously dispersed within a SWNT mesh of finite thickness. It is expected from previous experimental work [25] that the surface coverage of adsorbed enzyme will be relatively high, typically lying in the range 90-160 pmol cm⁻². Hence the mathematical model to be developed will consider both the transport of substrate and mediator in the solution filled pores between the nanotube strands to either the redox enzyme site or to the electrode surface, the enzyme/mediator and enzyme substrate reaction kinetics and the reaction kinetics of the mediator at the support electrode surface or at the nanotube sidewall. Furthermore the detailed relationship between the substrate reaction flux f_s and the observed flux f_x measured at the electrode is determined.

2. THEORETICAL MODEL

2.1 Model setup and general considerations

Our mathematical analysis will involve the following simplifications. We assume for simplicity that the mesh of carbon nanotubes immobilized on a conductive support electrode surface can be described in terms of a homogeneous slab of uniform thickness L . We also assume, unlike part 1 of the present series, that the redox enzyme is distributed homogeneously throughout the body of this slab with a concentration e_x . We denote the bulk concentration of substrate as s^∞ and that of oxidized redox mediator as a^∞ . We assume that both the substrate and oxidised redox mediator (such as oxygen) can diffuse through the external bathing solution and rapidly partition into the nanotube/enzyme layer with partition coefficients designated as κ_s , κ_A respectively. For ease of analysis we neglect the effect of mediator and substrate diffusion in the solution adjacent to the nanotube layer and therefore assume that at $x = L$, $s_L = \kappa_s s^\infty$, $a_L = \kappa_A a^\infty$.

We can visualise two distinct situations. The first occurs when the nanotube sample is conducting. This situation is illustrated in figure 2. The second (outlined schematically in figure 3) pertains when the nanotube sample is not so conducting. In the first case the reduced mediator reacts along the length of the nanotube strands. In the second the reduced mediator is required to diffuse to the support electrode surface and react there.

We assume that the reaction between oxidized enzyme and substrate proceeds via Michaelis-Menten kinetics. The reduced enzyme is regenerated via reaction with the oxidized mediator in the film. This reaction is assumed to proceed via simple bimolecular reaction kinetics, although it is quite possible that the reaction between oxidized mediator and reduced enzyme can also involve adduct formation and thus involve a Michaelis-Menten type mechanism. This particular possibility was considered in the first paper of this series [112].

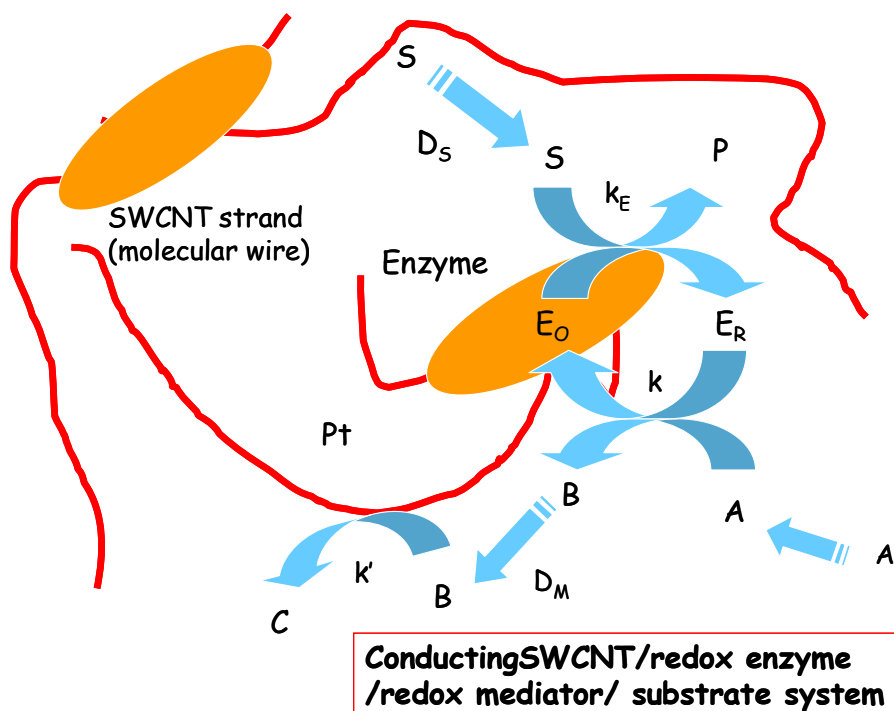


Figure 2. Schematic representation of reaction and diffusion of substrate and mediator within an immobilized nanotube mesh. The nanotube acts as a molecular wire and the mediator reacts along the nanotube surface.

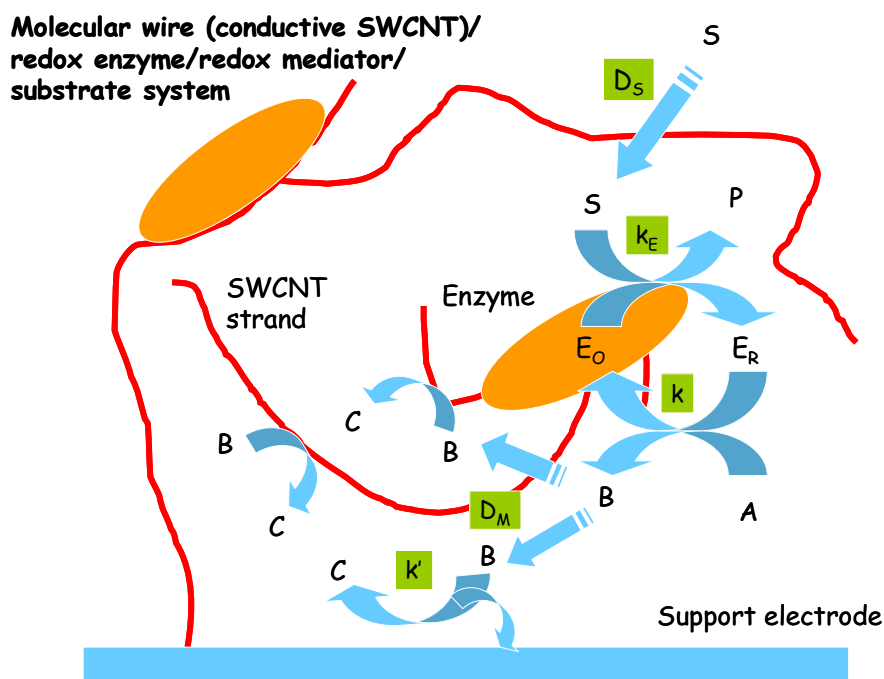
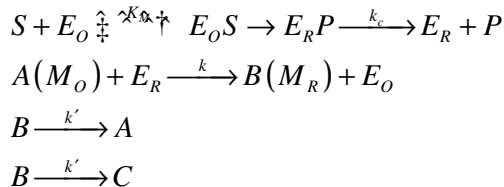


Figure 3. Schematic representation of reaction and diffusion of substrate and mediator within an immobilized nanotube mesh. The nanotube acts as a molecular wire and the mediator reacts at the underlying support electrode surface.

We therefore describe the reaction sequence in terms of the ‘ping-pong’ mechanism.



where S, P represent the substrate and product species respectively, E_O , E_R denote the oxidized and reduced forms of the redox enzyme and A, B denote the oxidized (M_O) and reduced (M_R) forms of the redox mediator respectively. Typical examples of the latter might be O_2/H_2O_2 [66] or benzoquinone/hydroquinone [71] respectively. Note that the reduced form of the mediator may react either to regenerate the oxidized form A or be reduced further to form a product C. The specifics of the reaction will depend on the electrode potential applied to the modified electrode. In either case the kinetics of the heterogeneous electron transfer reaction is quantified via the heterogeneous rate constant k' which will be potential dependent and follow Butler-Volmer kinetics. We assume that the SWNT mesh immobilized on the support electrode surface is very open and porous and the diffusion of substrate and redox mediator species in the nanotube layer is described by the diffusion coefficients D_S and $D_M = D_A = D_B$ respectively. The Michaelis Menten enzyme kinetics are described in terms of the Michaelis constant K_M and the catalytic rate constant k_c respectively.

As noted in part 1 of this series [112] the enzyme/substrate reaction and the rate of the enzyme/mediator reaction are assumed to give rise to a substrate flux f_s which is measured in the usual units of amount transformed per unit area per unit time ($\text{mol cm}^{-2} \text{s}^{-1}$). This will be related in some defined manner to the observed flux f_Σ which is measured at the electrode and is related to the current flowing via the expression:

$$f_\Sigma = \frac{i}{nFA} \quad (1)$$

where n, F and A denote the number of electrons transferred, the Faraday constant and the electrode geometric area respectively. The exact relationship depends on whether the mediator reacts along the nanotube strand or at the underlying support electrode. In the first case $f_\Sigma = f_s$, whereas in the second situation the net flux will differ from the substrate flux in a well defined manner. We will consider both of these cases in the present paper. We assume that the heterogeneous rate constant k' is well described by the Butler-Volmer equation:

$$k' = k^0 \exp[\pm \beta \xi] = k^0 \exp\left[\pm \frac{\beta F}{RT} (E - E^0)\right] \quad (2)$$

where $\xi = \frac{F}{RT} (E - E^0)$ denotes a normalised potential, β is the symmetry factor (typically for simple ET reactions $\beta = 1/2$) and the other symbols have their usual meanings. When the heterogeneous rate

constant is very large then the ratio of the reduced to oxidized mediator concentrations at the layer/support electrode interface will be related via the Nernst equation.

Furthermore if δ denotes the diffusion layer thickness then for distances $x > \delta$ we note that $b = 0$, $s = s^\infty$, $a = a^\infty$. Hence for distances greater than the diffusion layer thickness we propose that the concentration of reduced redox mediator is zero and that the concentration of substrate and oxidized mediator species admit their bulk values. When the mediator reacts at the underlying support electrode surface the net flux is given by:

$$f_\Sigma = D_B \left(\frac{db}{dx} \right)_0 = k'b_0 \quad (3)$$

In contrast when the mediator reacts along the nanotube strand we can write:

$$f_\Sigma = f_S = D_S \left(\frac{ds}{dx} \right)_{x=L} = \int_{x=0}^{x=L} ks(x) dx \quad (4)$$

Where we note that the rate constant k (units: s^{-1}) is given by: $k = (k_c/K_M) e_\Sigma = k_U e_\Sigma$ where k_c denotes the catalytic rate constant and K_M is the Michaelis constant for the immobilized redox enzyme. Furthermore $k_U = k_c/K_M$ and e_Σ denotes the total enzyme concentration.

2.2. Definition of the boundary value problem

We first focus attention on the fate of the reduced mediator species B. We can assume that the reduced mediator species B diffuses through the nanotube film to the support electrode where it is detected via direct electron transfer quantified by the heterogeneous electrochemical rate constant k' and it is generated in the nanotube layer via reaction between the oxidized mediator species A and the reduced enzyme E_R . The latter is quantified by a bimolecular rate constant k . Hence the pertinent reaction/diffusion equation for the reduced mediator species in the layer is given by (assuming steady state conditions):

$$D_B \frac{d^2b}{dx^2} + k e_R a = 0 \quad (5)$$

In the latter expression e_R and a denote the concentrations of reduced enzyme and oxidized mediator species within the nanotube layer. Furthermore for the substrate species S we need to consider diffusion of S in the film described by a diffusion coefficient D_S and subsequent reaction between S and oxidized enzyme E_O of concentration e_O :

$$D_S \frac{d^2s}{dx^2} - k_E e_O s = 0 \quad (6)$$

In the latter expression we note that the rate constant describing the reaction between oxidized enzyme and substrate is given by:

$$k_E = \frac{k_c}{K_M + s} \quad (7)$$

Now we note that if steady state conditions pertain:

$$\frac{de_O}{dt} = kae_R - k_E e_O s \cong 0 \quad (8)$$

And so the concentration of reduced enzyme is given by:

$$e_R = \frac{k_E s e_O}{ka} \quad (9)$$

Now we also note that :

$$e_O + e_R = e_\Sigma \quad (10)$$

From en.7, eqn.9 and eqn.10 we can show that:

$$\begin{aligned} e_R &= \frac{k_E s e_\Sigma}{ka} \left\{ 1 + \frac{k_E s}{ka} \right\}^{-1} \\ &= \frac{k_E s e_\Sigma}{ka + k_E s} = \frac{k_c e_\Sigma s}{ka(K_M + s) + k_c s} \end{aligned} \quad (11)$$

Hence eqn.5 transforms to

$$D_B \frac{d^2 b}{dx^2} + \frac{kak_c e_\Sigma s}{ka(s + K_M) + k_c s} = 0 \quad (12)$$

Also by noting that $k_E e_O s = kae_R$ then eqn.6 transforms to

$$D_S \frac{d^2 s}{dx^2} - kae_R = 0 \quad (13)$$

And using the result presented in eqn.11 we finally obtain

$$D_S \frac{d^2 s}{dx^2} - \frac{kak_c e_\Sigma s}{ka(s + K_M) + k_c s} = 0 \quad (14)$$

We note that eqn.12 and eqn.14 provide the fundamental description for reaction and diffusion of mediator and substrate within the nanotube layer and are similar in form to expressions previously derived by Bartlett and co-workers [65-68] for enzyme transport and kinetics within electroactive polymer materials.

These expressions must be solved subject to the following boundary conditions. If the reduced mediator species B reacts on the SWCNT fibers throughout the thickness L of the layer then we have:

$$\begin{aligned} x = 0, \quad \frac{ds}{dx} &= 0 \\ x = L, \quad s_L &= \kappa_S s^\infty \\ f_S &= D_S \left(\frac{ds}{dx} \right)_{x=L} \end{aligned} \quad (15)$$

Alternatively, if the reduced mediator B reacts at the support electrode surface then we solve eqn.14 for $s(x)$ and use the latter result in eqn.12 and then solve the latter reaction/diffusion equation subject to the latter boundary conditions:

$$\begin{aligned}
 x=0, \quad b=b_0=f_\Sigma/k', \quad f_\Sigma=f_B=D_B\left(\frac{db}{dx}\right)_{x=0} \\
 x=L, \quad b=b_L=0, \quad a=a_L=\kappa_A a^\infty
 \end{aligned}
 \tag{16}$$

In the latter expressions we have neglected concentration polarization of A and B in the solution adjacent to the nanotube layer. We also assume that the concentration of oxidized mediator has a uniform value given by $a = \kappa_A a^\infty$ throughout the nanotube film.

2.3. Transformation to non-dimensional variables

We [47] and others [56,68] have noted in previous publications that resolution of a complex boundary value problem of the type outlined in section 2.2 is best accomplished if the pertinent reaction diffusion equations and boundary conditions are transformed into non-dimensional format. This procedure ensures that the mathematical expressions are cast into a form that makes identification of suitable approximations more transparent. The introduction of characteristic dimensionless parameters related to the fundamental physical processes occurring in the system also enables the formulation of suitable limiting expressions for the reaction flux the predictions of which may be compared directly with experimental measurements.

We introduce the following dimensionless distance and concentration variables:

$$\chi = \frac{x}{L} \quad u = \frac{s}{\kappa_S s^\infty} \quad v = \frac{b}{\kappa_A a^\infty}
 \tag{17}$$

We also introduce the saturation parameter α as follows [47]:

$$\alpha = \frac{\kappa_S s^\infty}{K_M}
 \tag{18}$$

The latter parameter provides a measure of the degree of substrate unsaturation/saturation within the nanotube layer. When $\alpha \ll 1$, $s \ll K_M$ and the enzyme/substrate reaction kinetics within the layer is unsaturated (rate depends linearly on substrate concentration), whereas in contrast when $\alpha \gg 1$, $s \gg K_M$ the enzyme/substrate reaction kinetics are saturated (rate independent of substrate concentration). These two limits define Michaelis-Menten enzyme kinetics.

There are various ways [47,68] in which the reaction/diffusion equations may be made dimensionless. In the present formulation detailed analysis indicates that the following expressions may be obtained:

$$\frac{d^2 u}{d\chi^2} - \frac{\gamma_S F(u)}{1 + \kappa F(u)} = 0
 \tag{19}$$

$$\frac{d^2 v}{d\chi^2} + \frac{\gamma_M F(u)}{1 + \kappa F(u)} = 0
 \tag{20}$$

In the latter expressions we introduce the saturation function $F(u)$ as:

$$F(u) = \frac{u}{1 + \alpha u}
 \tag{21}$$

where we note that [47] $\alpha u = s/K_M$ quantifies the degree of unsaturation/saturation. We note that when $\alpha u \ll 1$, $F(u) \cong u$ and we have unsaturated enzyme kinetics. In contrast when $\alpha u \gg 1$, $F(u) \cong \frac{1}{\alpha}$ and we have saturated enzyme kinetics. Furthermore we have introduced the following reaction/diffusion parameters for substrate and redox mediator respectively:

$$\gamma_S = \frac{f_{SE}}{f_{SD}} = \frac{(k_c/K_M)e_{\Sigma}L\kappa_S s^{\infty}}{D_S\kappa_S s^{\infty}/L} \quad (22)$$

$$\gamma_M = \frac{f_{SE}}{f_{MD}} = \frac{(k_c/K_M)e_{\Sigma}L\kappa_S s^{\infty}}{D_M\kappa_A a^{\infty}/L} \quad (23)$$

Also we define a kinetic competition parameter κ as follows:

$$\kappa = \frac{f_{SE}}{f_{ME}} = \frac{(k_c/K_M)e_{\Sigma}L\kappa_S s^{\infty}}{ke_{\Sigma}L\kappa_A a^{\infty}} \quad (24)$$

We note that the parameter γ_S compares the rate of reaction between substrate and oxidized enzyme defined by the flux term f_{SE} with the rate of substrate diffusion through the nanotube layer defined by the flux term f_{SD} . In an analogous manner the parameter γ_M compares the rate of reaction between substrate and oxidized enzyme defined by the flux term f_{SE} with the rate of mediator diffusion through the nanotube layer defined by the flux term f_{MD} . Finally the parameter κ defines the balance between two kinetic reaction rates in the film: the oxidized enzyme/substrate flux f_{SE} (defined by the unsaturated bimolecular rate constant $k_U = k_c/K_M$) and the reduced enzyme/oxidized mediator flux f_{ME} (defined by the bimolecular rate constant k). When $\kappa \ll 1$, $f_{SE} \ll f_{ME}$ and the reaction kinetics are limited by the reaction between oxidized enzyme and substrate. The film consists of the oxidized enzyme only. In contrast when $\kappa \gg 1$, $f_{SE} \gg f_{ME}$ and the kinetics are limited by that of reaction between the reduced enzyme and oxidized mediator species A to regenerate the catalytically active oxidized enzyme. Hence the film consists of reduced enzyme only.

The pertinent boundary conditions for a conducting SWNT ensemble where the mediator reacts on the nanotube sidewall is:

$$\begin{aligned} \chi=0 \quad \left(\frac{du}{d\chi} \right)_0 &= 0 \\ \chi=1 \quad u &= 1 \end{aligned} \quad (25)$$

And the substrate flux is given by:

$$\Psi_S = \frac{f_S}{f_{SD}} = \frac{f_S}{\kappa_S D_S s^{\infty}/L} = \left(\frac{du}{d\chi} \right)_1 = \int_0^1 \gamma_S u(\chi) d\chi \quad (26)$$

When the nanotube ensemble is not so conducting then the current measures the reaction of the redox mediator at the underlying support electrode and the relevant boundary conditions in normalized form is given by:

$$\begin{aligned} \chi=0 \quad v &= v_0 \\ \chi=1 \quad v &= 0 \end{aligned} \quad (27)$$

And the net observed flux is given by:

$$\Psi_{\Sigma} = \zeta v_0 = \left(\frac{dv}{d\chi} \right)_0 \quad (28)$$

Where we note that:

$$\zeta = \frac{k'}{D_M/L} \quad (29)$$

This is a parameter which directly compares the heterogeneous electrochemical rate constant for reduced mediator transformation to product at the support electrode to the diffusive rate constant for reduced mediator transport to the support electrode surface.

2.4. Relationship between observed flux and substrate flux

We now derive a relationship between the observed flux Ψ_{Σ} and the substrate reaction flux Ψ_s . In general these will not be equal [112] and indeed $\Psi_{\Sigma} < \Psi_s$.

We begin by adding eqn.19 and eqn.20 to obtain:

$$\frac{d^2v}{d\chi^2} = -\frac{\gamma_M}{\gamma_s} \frac{d^2u}{d\chi^2} \quad (30)$$

Integrating the latter expression over the dimension of the nanotube layer between the limits of 0 and 1 we obtain:

$$\left(\frac{dv}{d\chi} \right)_1 - \left(\frac{dv}{d\chi} \right)_0 = -\frac{\gamma_M}{\gamma_s} \left\{ \left(\frac{du}{d\chi} \right)_1 - \left(\frac{du}{d\chi} \right)_0 \right\} \quad (31)$$

Now since we assume that the substrate does not react directly at the underlying support electrode surface then $\left(\frac{du}{d\chi} \right)_0 \equiv 0$. Furthermore we note that $\left(\frac{du}{d\chi} \right)_1 = \Psi_s$, $\left(\frac{dv}{d\chi} \right)_0 = \Psi_{\Sigma}$ and so eqn.31 reduces to:

$$\Psi_{\Sigma} = \frac{\gamma_M}{\gamma_s} \Psi_s + \left(\frac{dv}{d\chi} \right)_1 \quad (32)$$

This expression is equivalent to eqn.A3 in the first paper of this series [112]. As first noted by Bartlett and co-workers [68] there are three ways in which the reduced mediator is lost from the film. First it can be turned over at the electrode. Second it can escape into the bulk solution. Third it may be turned over by the substrate. The first two processes are described by the fluxes of mediator at the electrode surface and the film/solution interface respectively. With no enzyme catalyzed reaction occurring these two fluxes must be equal for steady state to be attained. The difference between these two fluxes is therefore due to turnover of mediator by the substrate. Now the substrate can only enter the nanotube film at the layer/solution interface, and be consumed by reaction with the mediator, since it has zero flux at the electrode surface. These two processes must therefore balance at steady state. Since the enzyme is only present in small catalytic quantities, the rate of enzyme catalysed

consumption of substrate is equal to that of the mediator. We therefore note that at steady state the flux of substrate into the film must therefore be equal to the difference between the fluxes of mediator at the electrode and at the film/solution interface and from eqn.32 we can write:

$$\Psi_s = \frac{\gamma_s}{\gamma_M} \left\{ \Psi_\Sigma - \left(\frac{dv}{d\chi} \right)_1 \right\} \quad (33)$$

2.5. The thin film limit

It is clear that exact solutions of the u and v master equations presented in eqn.19 and eqn.20 cannot be derived for all values of α and κ . This is because the kinetic terms in the expressions are non-linear. In order to obtain mathematical solutions to these master equations it is necessary to simplify them. One particular strategy is to examine the so called ‘thin film’ limit. Here we assume that substrate diffusion is so rapid that there are no reaction layers within the film. Under these circumstances we set $u \cong 1$ and $v \cong 1$, so the concentrations of substrate and mediator will be uniform throughout the layer.

We initially examine eqn.19 and consider the situation pertaining when the nanotube film is conducting. Setting $u \cong 1$ in eqn.19 and noting in this circumstance that $F(u) \cong \frac{1}{1+\alpha}$ we get:

$$\frac{d^2u}{d\chi^2} - \frac{\gamma_s/(1+\alpha)}{1+\kappa/(1+\alpha)} = 0 \quad (34)$$

This expression can be further simplified to:

$$\frac{d^2u}{d\chi^2} - \frac{\gamma_s}{1+\alpha+\kappa} = 0 \quad (35)$$

We can readily show by direct integration that the normalized substrate flux is given by:

$$\Psi_s = \left(\frac{du}{d\chi} \right)_1 = \frac{\gamma_s}{1+\alpha+\kappa} \quad (36)$$

We examine the limits of large and small α corresponding to substrate saturation and unsaturation respectively. First when $\alpha \gg 1$ or $s \gg K_M$ we note that eqn.36 reduces to:

$$\Psi_s \cong \frac{\gamma_s}{\alpha+\kappa} \quad (37)$$

The latter expression can be reduced to simpler representations depending on the balance between α and κ . For example when $\alpha \gg \kappa$ eqn.37 reduces to:

$$\Psi_s \cong \frac{\gamma_s}{\alpha} \quad (38)$$

If we insert the values for each of the dimensionless parameters obtained from eqn.18, eqn.24 and eqn.26 into eqn.38 we immediately obtain the following approximate expression for the substrate reaction flux:

$$f_s \cong k_c e_\Sigma L \quad (39)$$

This expression describes the situation of rate determining decomposition of the ES complex which will pertain when the enzyme kinetics is saturated. Here the flux is independent both of the substrate and oxidized mediator concentration. The flux is first order with respect to layer thickness and enzyme concentration. This will be labeled case III.

In contrast when $\alpha \ll \kappa$ corresponding to the situation where $\alpha \gg 1$ and so κ is very large indeed implying that $f_{SE} \gg f_{ME}$ then eqn.37 reduces to:

$$\Psi_s \cong \frac{\gamma_s}{\kappa} \quad (40)$$

And again from eqn.24 and eqn.26 we get that the substrate reaction flux is:

$$f_s \cong k\kappa_A e_{\Sigma} L a^{\infty} \quad (41)$$

Here the flux is independent of substrate concentration and is first order with respect to enzyme concentration, oxidized mediator concentration and layer thickness. This is designated case V and corresponds to rate determining reaction between oxidized mediator and reduced enzyme. The regeneration of the catalytically active oxidized enzyme is rate determining.

Turning to the situation when the saturation parameter is small such that $\alpha \ll 1$ then $s \ll K_M$ and we consider the case when the substrate concentration is low. This is the important case for amperometric detection. Under such conditions eqn.36 reduces to:

$$\Psi_s \cong \frac{\gamma_s}{1 + \kappa} \quad (42)$$

Here we can again consider two limits. First when $\kappa \ll 1$ which corresponds to the situation where $f_{SE} \ll f_{ME}$ then eqn.42 reduces to:

$$\Psi_s \cong \gamma_s \quad (43)$$

Transforming to an expression for the substrate flux affords:

$$f_s \cong \left(\frac{k_c}{K_M} \right) e_{\Sigma} L \kappa_s s^{\infty} \quad (44)$$

This situation describes rate determining bimolecular reaction between substrate and oxidized enzyme (unsaturated enzyme kinetics). This is case I. Here the substrate flux and hence the current is first order with respect to substrate concentration, enzyme concentration and layer thickness. When $\kappa \gg 1$ eqn.42 reduces to eqn.40 and the substrate flux is defined in terms of eqn.41. Again we regain case V and have rate determining regeneration of the oxidized enzyme. Hence case V pertains for all values of the substrate concentration.

We now consider eqn.20 which pertains when the nanotube layer is not so conducting. Again $F(u) \cong \frac{1}{1 + \alpha}$ and eqn.20 reduces to:

$$\frac{d^2 v}{d\chi^2} + \frac{\gamma_M}{1 + \alpha + \kappa} = 0 \quad (45)$$

This expression may be integrated once to yield:

$$\frac{dv}{d\chi} = -\frac{\gamma_M \chi}{1 + \alpha + \kappa} + A \quad (46)$$

And integrated again to produce

$$v = -\frac{\gamma_M \chi^2}{2(1 + \alpha + \kappa)} + A\chi + B \quad (47)$$

The integration constants A and B are evaluated from the pertinent boundary conditions. When $\chi = 0$ $v = v_0$ and so immediately $B = v_0$. Again when $\chi = 0$ $A = \left(\frac{dv}{d\chi}\right)_0 = \Psi_\Sigma = \zeta v_0$. Furthermore when $\chi = 1$ $v = v_1 = 0$ and eqn.47 reduces to:

$$v_0 = \frac{\gamma_M}{2(1 + \zeta)(1 + \alpha + \kappa)} \quad (48)$$

Hence the total flux is given by

$$\Psi_\Sigma = \zeta v_0 = \frac{\gamma_M}{2(1 + \zeta^{-1})(1 + \alpha + \kappa)} \quad (49)$$

Recalling eqn.36 we can readily show that $1/(1 + \alpha + \kappa) = \Psi_s/\gamma_s$ and hence eqn.49 transforms to:

$$\Psi_\Sigma = \frac{\gamma_M}{\gamma_s} \left\{ \frac{1}{2(1 + \zeta^{-1})} \right\} \Psi_s \quad (50)$$

Where we note that the loss factor is given by:

$$\zeta^{-1} = \frac{D_M/L}{k'} = \frac{D_M/L}{k^0} \exp[m\beta\xi] \quad (51)$$

Hence the loss factor defines the ratio between the rate of reduced mediator diffusion from the layer into the solution to the rate of reduced mediator chemical transformation at the electrode surface. It is also dependent on potential. The negative sign in eqn.51 refers to the reduced mediator undergoing an oxidation at the support electrode whereas the positive sign signifies that the electrode is polarized such that the reduced mediator will undergo further reduction. The expression outlined in eqn.50 is a general relationship between the observed flux and the substrate flux and is therefore of considerable utility. In general when the potential is set to extreme values $\exp[m\beta\xi] \rightarrow 0$ and the following relation pertains between the corresponding limiting flux values:

$$\Psi_{\Sigma,L} = \frac{\gamma_M}{\gamma_s} \frac{\Psi_{s,L}}{2} \quad (52)$$

We note that $r = \frac{\gamma_M}{\gamma_s} = \frac{f_{SD}}{f_{MD}}$ defines the ratio of the substrate to mediator diffusive fluxes in the film. It is logical that the observed flux will also depend on this quantity. We illustrate in figure 4 a plot of the ratio Ψ_Σ/Ψ_s as function of the parameter ζ for various values of the ratio $r = \frac{\gamma_M}{\gamma_s} = \frac{f_{SD}}{f_{MD}}$.

It is clear that for any value of the ratio $r = \frac{\gamma_M}{\gamma_S} = \frac{f_{SD}}{f_{MD}}$, as the rate of mediator loss via electrochemical transformation at the support electrode/film interface increases (by increasing the potential applied to the electrode for example) compared with the rate of loss of mediator from the film via diffusion across the film/solution interface increases, the net flux approaches that due to substrate reaction. Furthermore the result predicted by eqn.52 is confirmed when the value of ζ is large which it will be at high potential : a constant plateau region is observed.

The expression presented in eqn.50 is also useful since it immediately enables us to evaluate the net flux for the three limiting kinetic situations considered previously for the situation where the observed current arises from reaction of the reduced mediator at the support electrode surface. When $\alpha \ll 1$ we recall that $\Psi_s \cong \frac{\gamma_S}{1+\kappa}$, and so the net flux is

$$\Psi_\Sigma = \frac{\gamma_M}{\gamma_S} \left\{ \frac{1}{2(1+\zeta^{-1})} \right\} \Psi_s \cong \frac{\gamma_M}{2(1+\zeta^{-1})} \left\{ \frac{1}{1+\kappa} \right\} \quad (53)$$

Hence for case I, corresponding to the case where $\alpha \ll 1$, $\kappa \ll 1$, the corresponding expression for the net flux is:

$$\Psi_\Sigma = \frac{\gamma_M}{\gamma_S} \left\{ \frac{1}{2(1+\zeta^{-1})} \right\} \Psi_s \cong \frac{\gamma_M}{2(1+\zeta^{-1})} \quad (54)$$

Or

$$f_\Sigma \cong \left\{ \frac{1}{2(1+\zeta^{-1})} \right\} \left(\frac{k_c}{K_M} \right) e_\Sigma L \kappa_s s^\infty \quad (54)$$

Which is rate determining unsaturated enzyme kinetics. When $\kappa \gg \alpha$, $\kappa \gg 1$, $\alpha \ll 1$, eqn.53 reduces to:

$$\Psi_\Sigma \cong \frac{\gamma_M}{2(1+\zeta^{-1})\kappa} \quad (55)$$

This defines kinetic case V valid for $s \ll K_M$. And hence we note

$$f_\Sigma \cong \frac{1}{2(1+\zeta^{-1})} k e_\Sigma L \kappa_A a^\infty \quad (56)$$

Hence the regeneration of the oxidized enzyme is rate determining.

In contrast when $\alpha \gg 1$ we get the two further cases. When $\alpha \gg 1$, $\kappa \ll 1$, $\alpha \gg \kappa$, case

III, we note that $\Psi_s \cong \frac{\gamma_S}{\alpha}$ and so the net flux becomes

$$\Psi_\Sigma = \frac{\gamma_M}{\gamma_S} \left\{ \frac{1}{2(1+\zeta^{-1})} \right\} \Psi_s \cong \frac{\gamma_M}{2(1+\zeta^{-1})\alpha} \quad (57)$$

And the net flux is

$$f_{\Sigma} \cong \frac{1}{2(1+\zeta^{-1})} k_c e_2 L \tag{58}$$

Which corresponds to rate determining saturated enzyme kinetics.

Finally for $\alpha \gg 1$, $\kappa \gg 1$, $\kappa \gg \alpha$ we enter the region defining kinetic case V and $\Psi_s \cong \frac{\gamma_s}{\kappa}$ so the net flux again takes the form outlined in eqn.55 and eqn.56. And the regeneration of the oxidized enzyme is again rate determining. Hence enzyme regeneration can be rate determining over the entire substrate concentration range.

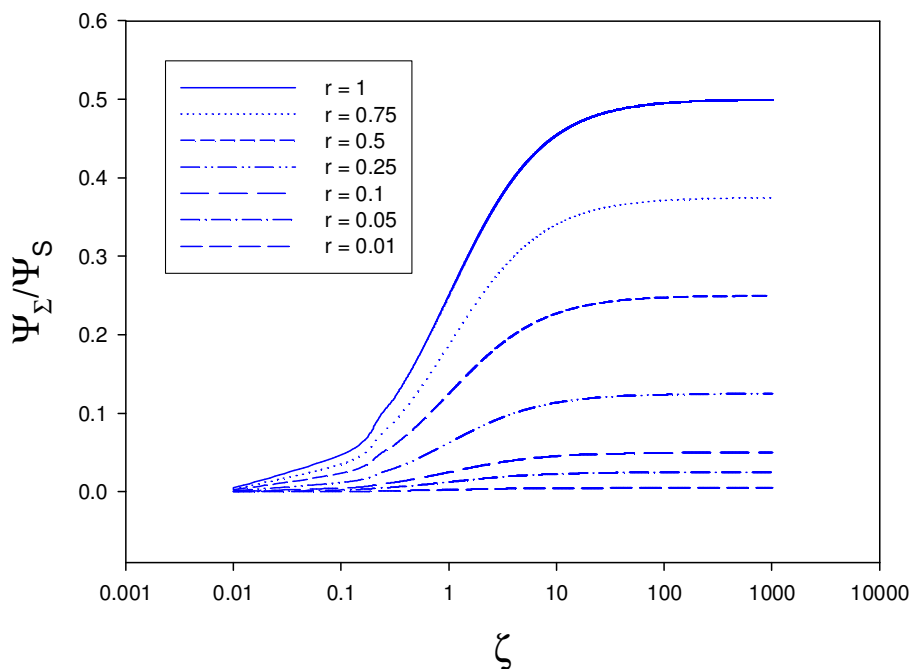


Figure 4. Variation of flux ratio with ζ parameter calculated via eqn.50 for various defined values of the substrate/mediator transport flux ratio r .

We conclude that significant insights into the transport and kinetics can be extracted via use of the thin layer approximation. We now progress and extend the analysis to consider the case where the immobilized enzyme layer is of finite thickness. We will show that three further distinct kinetic cases can be identified.

2.5. Conductive matrix: finite thickness

We now relax the thin film condition and assume that the concentration polarization of substrate must be considered within the immobilized enzyme layer. Hence eqn.19 must be solved. If we assume unsaturated conditions then $\alpha u \ll 1$, $F(u) \cong u$ and eqn.19 reduces to:

$$\frac{d^2u}{d\chi^2} - \frac{\gamma_s u}{1 + \kappa u} = 0 \quad (59)$$

When $\kappa u \ll 1$, then $1 + \kappa u \cong 1$ and the u-equation reduces to

$$\frac{d^2u}{d\chi^2} - \gamma_s u = 0 \quad (60)$$

This expression may be readily integrated to yield

$$u = A_1 \cosh[\sqrt{\gamma_s} \chi] + B_1 \sinh[\sqrt{\gamma_s} \chi] \quad (61)$$

$$\frac{du}{d\chi} = \sqrt{\gamma_s} A_1 \sinh[\sqrt{\gamma_s} \chi] + \sqrt{\gamma_s} B_1 \cosh[\sqrt{\gamma_s} \chi]$$

When $\chi = 0$ $\frac{du}{d\chi} = 0$, hence $B_1 = 0$. Also when $\chi = 1$ $u = 1$ and so $A_1 = \frac{1}{\cosh[\sqrt{\gamma_s}]}$. Hence

the substrate concentration profile through the layer is given by:

$$u(\chi) = \frac{\cosh[\sqrt{\gamma_s} \chi]}{\cosh[\sqrt{\gamma_s}]} \quad (62)$$

Furthermore the normalized substrate flux is given by:

$$\Psi_s = \left(\frac{du}{d\chi} \right)_1 = \sqrt{\gamma_s} \tanh[\sqrt{\gamma_s}] \quad (63)$$

This result has been derived in a previous analysis [47,59] performed for reaction/diffusion with Michaelis-Menten kinetics for substrate reaction within an electronically conducting polymer thin film. We can consider two distinct limits. First when $\sqrt{\gamma_s} \ll 1$ then $f_{SE} \ll f_{SD}$ and substrate/enzyme unsaturated reaction kinetics will be much slower than the rate of substrate diffusion through the film which will be fairly rapid. In other words the layer thickness is very much less than the kinetic length of the substrate. Then we assume that $\tanh[\sqrt{\gamma_s}] \cong \sqrt{\gamma_s}$ and so the normalized substrate flux admits the following form:

$$\Psi_s \cong \gamma_s \quad (43)$$

This of course is case I already discussed in the thin film limit. When substrate diffusion is very rapid we effectively have the latter limit so our result is not to be unexpected. Again the flux will be given by eqn.44 corresponding to rate determining unsaturated Michaelis Menten kinetics occurring within the bulk of the immobilized enzyme layer. This result will be valid when the mediator/enzyme flux is also large. As noted in eqn.44 the reaction flux and hence the current is first order with respect to substrate concentration, enzyme concentration and layer thickness. Here increasing the film thickness or enzyme loading increases the current because the reaction of substrate occurs uniformly throughout the layer. In contrast when $\sqrt{\gamma_s} \gg 1$ then $f_{SE} \gg f_{SD}$ and substrate diffusion through the film will be slower than the substrate/enzyme reaction kinetics. Hence the layer thickness is very much larger than the kinetic length. Under these circumstances we note that $\tanh[\sqrt{\gamma_s}] \cong 1$ and the normalized substrate flux reduces to:

$$\Psi_s \cong \sqrt{\gamma_s} \quad (64)$$

This is a new case which we denote as case II. We can readily show that the substrate flux is given by:

$$f_s \cong \sqrt{\left(\frac{k_c}{K_M}\right)} D_s e_{\Sigma} \kappa_s s^{\infty} \quad (65)$$

Here we note that reaction between substrate and enzyme is rate limiting and occurs in a region located in the outer edge of the film. This case will occur when the diffusivity of the substrate is relatively low or when the substrate only diffuses a short distance into the layer before it reacts with the enzyme in a thin reaction layer near the film/solution interface. This will occur when the reaction between enzyme and substrate is favoured and so the kinetic length will be small. We note that under such circumstances in case II the substrate flux and hence the measured current is half order with respect to enzyme concentration, is independent of layer thickness and is first order with respect to substrate concentration characteristic of unsaturated Michaelis - Menten kinetics.

We can re-examine eqn.59 and attempt another method of solution which will be valid when $\gamma_s \gg 1$ and when $\kappa \cong 1$. We note the following identities:

$$\begin{aligned} \frac{du}{d\chi} \left\{ \frac{d^2u}{d\chi^2} \right\} &= \gamma_s \frac{du}{d\chi} \left(\frac{u}{1+\kappa u} \right) \\ \frac{d}{d\chi} \left\{ \frac{du}{d\chi} \right\}^2 &= 2 \left(\frac{du}{d\chi} \right) \frac{d^2u}{d\chi^2} \end{aligned} \quad (66)$$

Hence we note that

$$\begin{aligned} \frac{d}{d\chi} \left(\frac{du}{d\chi} \right)^2 &= 2\gamma_s \left(\frac{u}{1+\kappa u} \right) \frac{du}{d\chi} \\ d \left\{ \frac{du}{d\chi} \right\}^2 &= 2\gamma_s \left(\frac{u}{1+\kappa u} \right) du \end{aligned} \quad (67)$$

Integrating we get:

$$\left(\frac{du}{d\chi} \right)^2 = 2\gamma_s \int_0^u \frac{u}{1+\kappa u} du \quad (68)$$

Now we note that:

$$\int \frac{u}{1+\kappa u} du = \frac{u}{\kappa} - \frac{1}{\kappa^2} \ln(1+\kappa u) \quad (69)$$

Noting that when $u = 0$ $\frac{du}{d\chi} = 0$ and so from eqn.67 and eqn.68 we get:

$$\frac{du}{d\chi} = \sqrt{2\gamma_s \left\{ \frac{u}{\kappa} - \frac{1}{\kappa^2} \ln(1+\kappa u) \right\}} \quad (70)$$

Noting that $u = 1$ when $\chi = 1$ we finally derive an expression for the normalized substrate flux:

$$\Psi_s = \left(\frac{du}{d\chi} \right)_1 = \sqrt{\frac{2\gamma_s}{\kappa^2} \{ \kappa - \ln(1+\kappa) \}} \quad (71)$$

Now when $\kappa \ll 1$ then we can assume that $\ln(1+\kappa) \cong \kappa - \frac{\kappa^2}{2}$ and so eqn.71 reduces to $\Psi_s \cong \sqrt{2 \frac{\gamma_s \kappa^2}{\kappa^2} \frac{\kappa^2}{2}} = \sqrt{\gamma_s}$ which is eqn.64 again describing case II. Alternatively when $\kappa \gg 1$ we note that $\ln(1+\kappa) \cong \ln \kappa$ and assuming that $\kappa \gg \ln \kappa$ we get:

$$\Psi_s \cong \sqrt{\frac{2\gamma_s}{\kappa^2} (\kappa - \ln \kappa)} \cong \sqrt{\frac{2\gamma_s}{\kappa}} \tag{72}$$

This expression defines a new kinetic case which we label case VI. Here the substrate flux is given by:

$$f_s \cong \sqrt{2k\kappa_s D_s s^\infty \kappa_A^\infty e_\Sigma} \tag{73}$$

Here we note that the reaction flux is half order with respect to enzyme concentration, substrate concentration and mediator concentration and is zero order with respect to layer thickness.

We now consider the situation when $\alpha u \gg 1$. Under such conditions $1 + \alpha u \cong \alpha u$ and $F(u) \cong \frac{1}{\alpha}$ and the reaction/diffusion eqn.19 reduces to:

$$\frac{d^2u}{d\chi^2} - \frac{\gamma_s/\alpha}{1 + \kappa/\alpha} = 0 \tag{74}$$

Here we need to consider the situation where either $\kappa/\alpha \ll 1$ or $\kappa/\alpha \gg 1$. First when $\kappa/\alpha \ll 1$ eqn.74 reduces to:

$$\frac{d^2u}{d\chi^2} - \frac{\gamma_s}{\alpha} = 0 \tag{75}$$

This expression may be readily integrated twice to produce:

$$\begin{aligned} \frac{du}{d\chi} &= \frac{\gamma_s}{\alpha} \chi + A_2 \\ u(\chi) &= \frac{\gamma_s}{2\alpha} \chi^2 + A_2 \chi + B_2 \end{aligned} \tag{76}$$

Now when:

$$\begin{aligned} \chi = 0 \quad \frac{du}{d\chi} &= 0 \\ \chi = 1 \quad u = 1 \quad \Psi_s &= \left(\frac{du}{d\chi} \right)_1 \end{aligned} \tag{77}$$

And so we note that $A_2 = 0$ $B_2 = 1 - \frac{\gamma_s}{2\alpha}$. Hence the normalized flux is given by:

$$\Psi_s \cong \left(\frac{du}{d\chi} \right)_1 \cong \frac{\gamma_s}{\alpha} \tag{38}$$

Which is case III already discussed. This expression describes the situation of rate determining decomposition of the ES complex which will pertain when the enzyme kinetics is saturated. We recall that the substrate flux is given by $f_s \cong k_c e_\Sigma L$. Here the flux is independent both of the substrate and oxidized mediator concentration. The flux is first order with respect to layer thickness and enzyme

concentration. We can readily show that the substrate concentration profile within the layer is given by:

$$u(\chi) \cong 1 - \frac{\gamma_s}{2\alpha}(1 - \chi^2) \quad (78)$$

In contrast when $\kappa/\alpha \gg 1$ then $1 + \kappa/\alpha \cong \kappa/\alpha$ and eqn.74 reduces to:

$$\frac{d^2u}{d\chi^2} - \frac{\gamma_s}{\kappa} = 0 \quad (79)$$

Integrating twice we obtain:

$$\frac{du}{d\chi} = \frac{\gamma_s}{\kappa}\chi + A_3 \quad (80)$$

$$u(\chi) = \frac{\gamma_s}{2\kappa}\chi^2 + A_3\chi + B_3$$

Again using the boundary conditions outlined in eqn.77 we obtain that: $A_3 = 0$ $B_3 = 1 - \frac{\gamma_s}{2\kappa}$.

Hence the normalized flux is given by:

$$\Psi_s \cong \frac{\gamma_s}{\kappa} \quad (40)$$

This is case V corresponding to rate determining reaction between oxidized mediator and reduced enzyme. The regeneration of the catalytically active oxidized enzyme is rate determining. We recall that the substrate flux is given by $f_s \cong k\kappa_A e_2 La^\infty$. Here the flux is independent of substrate concentration and is first order with respect to enzyme concentration, oxidized mediator concentration and layer thickness. The reaction between oxidized mediator and reduced enzyme occurs throughout the film and so increases in direct proportion to increasing layer thickness. The flux is independent of substrate concentration since the enzyme kinetics with respect to the latter are saturated.

We need to consider one final possible kinetic situation. This is termed the moving boundary scenario. Here we assume that $\alpha \gg 1$ and γ_s is large. The immobilized enzyme layer may be decomposed into two regions labeled RI and RII. The outermost region RII is assumed saturated whereas the inner region RI is unsaturated. Hence in RI $\alpha u < 1$ and in RII $\alpha u > 1$. The line of demarcation between RI and RII is labeled $\chi = \chi_*$. Here we note that $\alpha u = 1$. Hence when $\chi_* = 0$ the entire layer is saturated whereas when $\chi_* = 1$ the entire layer is unsaturated as outlined in fig.5. Furthermore when $\chi = 0$, $du/d\chi = 0$ and when $\chi = 1$, $u = 1$ as before.

The strategy we will adopt is to evaluate the flux expressions in regions RI and RII and using the condition of flux matching at $\chi = \chi_*$ to obtain an expression for the limiting substrate flux. Now in region RI, $\alpha u < 1$ and we solve $\frac{d^2u}{d\chi^2} - \frac{\gamma_s u}{1 + \kappa u} = 0$, which for $\kappa \ll 1$ reduces to $\frac{d^2u}{d\chi^2} - \gamma_s u = 0$. This expression may be solved as before by noting that $\chi = 0$ $\frac{du}{d\chi} = 0$ and when $\chi = \chi_*$ $u = 1/\alpha$. Hence

we note that :

$$\left(\frac{du}{d\chi} \right)_{\chi=\chi_*} = \frac{\sqrt{\gamma_s}}{\alpha} \tanh \left[\sqrt{\gamma_s} \chi_* \right] \quad (81)$$

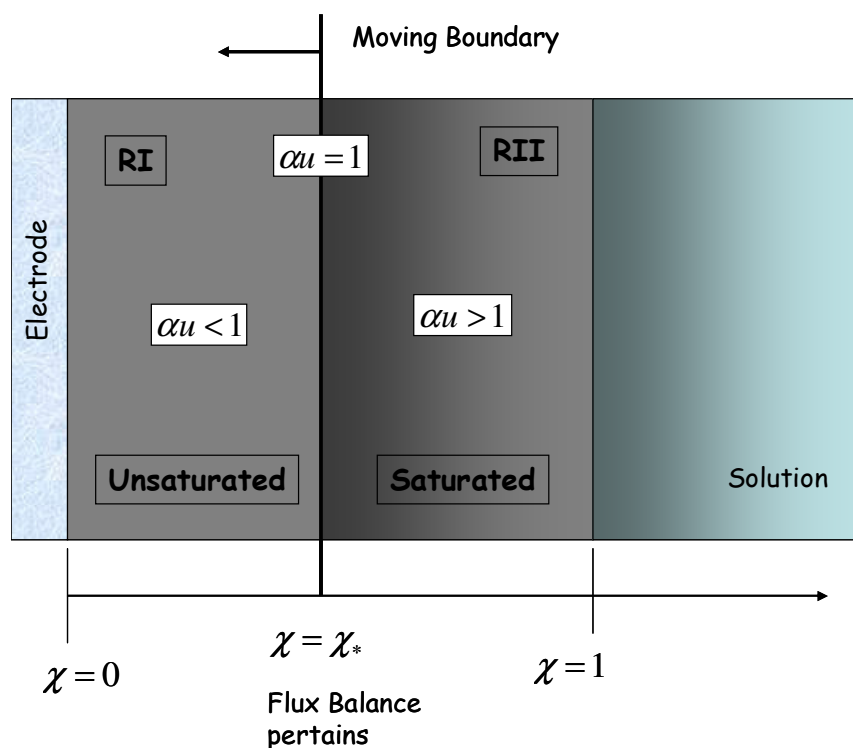


Figure 5. Delineation of two region approach : Moving Boundary case..

In region RII the pertinent reaction diffusion equation is given by $\frac{d^2u}{d\chi^2} - \frac{\gamma_s}{\alpha + \kappa} = 0$ or since $\kappa \ll \alpha$ which reduces to: $\frac{d^2u}{d\chi^2} - \frac{\gamma_s}{\alpha} = 0$. The latter expression integrates to at $\chi = \chi^*$:

$$\left(\frac{du}{d\chi}\right) = \frac{\gamma_s}{\alpha} \chi + A_4 \tag{82}$$

$$u = \frac{\gamma_s}{2\alpha} \chi^2 + A_4 \chi + B_4$$

Now using flux matching at $\chi = \chi^*$ in the first expression in eqn.82 and eqn.81 we get: $A_4 = \frac{\sqrt{\gamma_s}}{\alpha} \tanh[\sqrt{\gamma_s} \chi^*] - \frac{\gamma_s}{\alpha} \chi^*$. Furthermore the substrate flux is given by:

$$\Psi_s = \left(\frac{du}{d\chi}\right)_{\chi=1} = \frac{\gamma_s}{\alpha} + A_4 = \frac{\gamma_s}{\alpha} - \frac{\gamma_s}{\alpha} \chi^* + \frac{\sqrt{\gamma_s}}{\alpha} \tanh[\sqrt{\gamma_s} \chi^*] \tag{82}$$

Hence in order to evaluate the substrate flux we must initially evaluate χ^* . Using the second expression in eqn.82 at $\chi = 1$ we get : $1 = \frac{\gamma_s}{2\alpha} + A_4 + B_4$. Furthermore when $\chi = \chi^*$ $\alpha u = 1$, and so

$u = 1/\alpha$ and so $\frac{1}{\alpha} = \frac{\gamma_s}{2\alpha} \chi^{*2} + A_4 \chi^* + B_4$. Hence we note that

$B_4 = \frac{1}{\alpha} - \frac{\gamma_s}{2\alpha} \chi^{*2} - A_4 \chi^* = \frac{1}{\alpha} - \frac{\gamma_s}{2\alpha} \chi^{*2} - \frac{\sqrt{\gamma_s}}{\alpha} \tanh[\sqrt{\gamma_s} \chi^*] \chi^* + \frac{\gamma_s}{\alpha} \chi^{*2}$ Now when

$\gamma_s \gg 1$ $\tanh\left[\sqrt{\gamma_s}\chi^*\right] \cong 1$ and so we finally obtain that : $B_4 = \frac{1}{\alpha} + \frac{\gamma_s}{2\alpha}\chi^{*2} - \frac{\sqrt{\gamma_s}}{\alpha}\chi^*$. Gathering the latter information together we can readily show that χ^* obeys the following quadratic equation:

$$\chi^{*2} - 2\left(1 + \frac{1}{\sqrt{\gamma_s}}\right)\chi^* + \frac{2}{\gamma_s}(1 - \alpha) + \frac{2}{\sqrt{\gamma_s}} + 1 = 0 \quad (83)$$

Solving this equation affords:

$$\chi^* = 1 + \frac{1}{\sqrt{\gamma_s}} - \sqrt{\frac{2\alpha - 1}{\gamma_s}} \cong 1 - \sqrt{\frac{2\alpha}{\gamma_s}} + \frac{1}{\sqrt{\gamma_s}} \cong 1 - \sqrt{\frac{2\alpha}{\gamma_s}} \quad (84)$$

Where we recall that $2\alpha \gg 1$ and $\gamma_s \gg 1$. Hence we conclude that the condition for complete saturation within the film can be defined when the parameter γ_s is large. This occurs when $\chi^* = 0$ or when $\gamma_s = 2\alpha$. Hence the range of validity defining the mixed kinetics case is $1 < \alpha < \frac{\gamma_s}{2}$. Now recalling eqn.82 we note that:

$$\begin{aligned} \Psi_s &\cong \frac{\gamma_s}{\alpha} - \frac{\gamma_s}{\alpha}\chi^* + \frac{\sqrt{\gamma_s}}{\alpha} \\ &= \sqrt{\frac{2\gamma_s}{\alpha}} \end{aligned} \quad (85)$$

This is a new kinetic situation which we label case IV. Transforming into dimensioned quantities we can show that in case IV the substrate flux admits the following form:

$$f_s \cong \sqrt{2\kappa_s D_s k_c e_s s^\infty} \quad (86)$$

Hence the substrate flux is half order with respect to substrate and enzyme concentrations, is independent of layer thickness and mediator concentrations, and the enzyme-substrate kinetics is rate determining since $\kappa \ll 1$. The latter process occurs in a thin reaction layer near the surface of the film since γ_s is large.

2.6. Not so conductive matrix: finite thickness

We now examine the more complicated situation where the nanotube matrix is not so conductive and we have to use a low molecular mass, mobile redox mediator such as oxygen [66], benzoquinone [71] or ferrocenyl monocarboxylic acid to ensure efficient amperometric detection.. Here the reduced mediator B diffuses to the underlying support electrode surface where it undergoes reaction, either being re-oxidized to the A form again or undergoing further reduction to a product species C.

Again we need to solve eqn.19 and eqn.20 for substrate and mediator subject to the boundary conditions presented in eqn.16. We note that the solution of the master equation for substrate is initially solved and the resulting expression for the normalized substrate concentration, u, is inserted into eqn.20 and the latter expression integrated to obtain an expression for the observed flux Ψ_Σ .

We first examine the mediator reaction/diffusion master equation in the limit where $\alpha u \ll 1$. In this situation eqn.20 reduces to:

$$\frac{d^2v}{d\chi^2} + \frac{\gamma_M u}{1 + \kappa u} = 0 \quad (87)$$

However if we make the further assumption that $\kappa u \ll 1$ then eqn.87 reduces to

$$\frac{d^2v}{d\chi^2} + \gamma_M u = 0 \quad (88)$$

Where we recall that $\gamma_M = \frac{f_{SE}}{f_{MD}} = \frac{(k_c/K_M)e_\Sigma L \kappa_S s^\infty}{D_M \kappa_A a^\infty / L}$. Now u is obtained from a solution of eqn.59. We have previously shown that $u = \sec h\left[\sqrt{\gamma_S}\right] \cosh\left[\sqrt{\gamma_S}\chi\right]$ and so eqn.88 reduces to:

$$\frac{d^2v}{d\chi^2} + \gamma_M \sec h\sqrt{\gamma_S} \cosh\left[\sqrt{\gamma_S}\chi\right] = 0 \quad (89)$$

This expression may be readily integrated once to obtain:

$$\frac{dv}{d\chi} = -\frac{\gamma_M}{\sqrt{\gamma_S}} \sec h\sqrt{\gamma_S} \sinh\left[\sqrt{\gamma_S}\chi\right] + K_1 \quad (90)$$

And integrated again to yield

$$v(\chi) = -\frac{\gamma_M}{\gamma_S} \sec h\sqrt{\gamma_S} \left\{ \cosh\left[\sqrt{\gamma_S}\chi\right] - 1 \right\} + K_1\chi + K_2 \quad (91)$$

Since $v=0$ when $\chi=1$ then $K_1 + K_2 = \frac{\gamma_M}{\gamma_S} \left\{ 1 - \sec h\sqrt{\gamma_S} \right\}$. Also when $\chi=0$ $v=v_0$, and so $v_0 = K_2 = \frac{\Psi_\Sigma}{\zeta}$. Also we note that $\left(\frac{dv}{d\chi}\right)_0 = K_1 = \Psi_\Sigma$. Taking all of these observations into consideration one may immediately derive that the net normalized mediator flux measured at the support electrode surface is:

$$\Psi_\Sigma = \frac{\gamma_M/\gamma_S}{1 + \zeta^{-1}} \left\{ 1 - \sec h\sqrt{\gamma_S} \right\} \quad (92)$$

The latter when transformed to the observed reaction flux is given by:

$$f_\Sigma = \frac{\kappa_S D_S s^\infty / L}{1 + \frac{D_M / L}{k'}} \left\{ 1 - \sec h \left[\sqrt{\frac{k_U \kappa_S s^\infty e_\Sigma L}{\kappa_S D_S s^\infty / L}} \right] \right\} \quad (93)$$

The expression outlined in eqn.92 is presented in figure 6 below. We note that the computation is done by setting $\zeta^{-1} = \frac{D_M / L}{k'} = 0.1$ and by varying the value for $\gamma_M = f_{SE} / f_{MD}$. Hence under the conditions set mediator diffusion is rapid through the film and redox mediator turnover at the support electrode is much faster than mediator diffusion through the film. We plot normalized flux versus substrate reaction/diffusion parameter which represents the balance between substrate/enzyme reaction kinetics and substrate diffusion through the film.

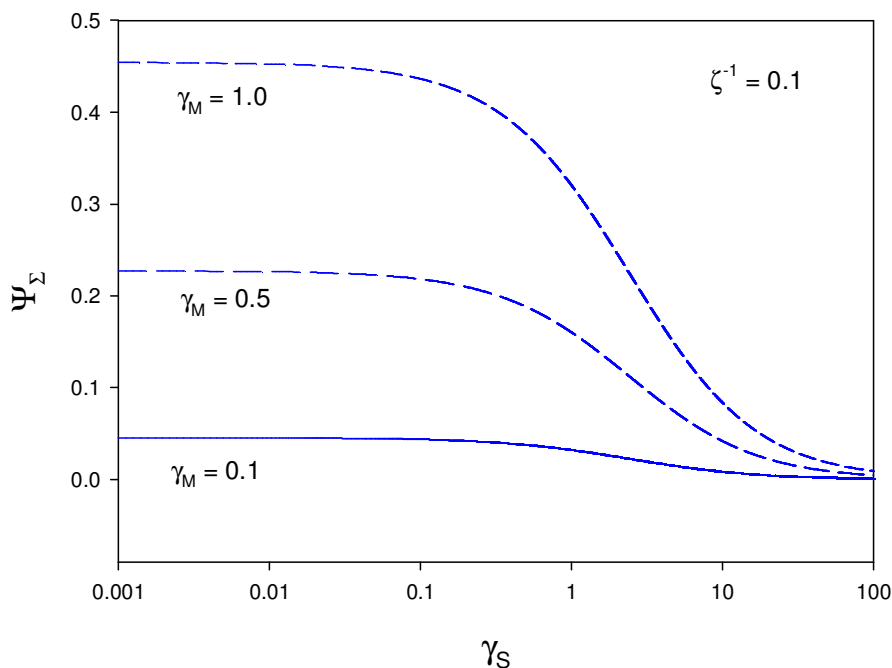


Figure 6. Variation of normalized flux versus substrate reaction/diffusion parameter defined via eqn.92.

It is clear from figure 6 that the normalized flux arising from redox mediator transformation measured at the support electrode surface decreases as the γ_s parameter increases corresponding to slower substrate diffusion and faster substrate reaction throughout the layer. This is to be expected since the substrate will not proceed far into the film before it undergoes reaction and much of the reduced mediator will be lost to the bulk solution from the film in these outer regions before it can travel and react at the support electrode surface.

We can also readily show that the mediator concentration profile within the nanotube layer is given by:

$$v(\chi) = \frac{\gamma_M}{\gamma_s} \left\{ 1 - \operatorname{sech} \sqrt{\gamma_s} \chi \right\} \left\{ \frac{1}{1 + \zeta} (1 + \zeta \chi) \right\} + \frac{\gamma_M}{\gamma_s} \operatorname{sech} \sqrt{\gamma_s} \chi \left\{ 1 - \cosh \left[\sqrt{\gamma_s} \chi \right] \right\} \quad (94)$$

Note that the loss factor is given by: $\zeta^{-1} = \frac{D_M/L}{k'} = \frac{D_M/L}{k^0} \exp[m\beta\xi]$. Now we can examine the limit of low and high substrate reaction diffusion parameter $\sqrt{\gamma_s}$. First when $\sqrt{\gamma_s} \ll 1$ corresponding to the situation where the layer thickness is very much less than the kinetic length of the substrate then $f_{SE} \ll f_{SD}$ and substrate/enzyme unsaturated reaction kinetics will be much slower than the rate of substrate diffusion through the film which will be fairly rapid.. Under these circumstances we approximate $\operatorname{sech} \sqrt{\gamma_s} \chi \cong 1 - \frac{\gamma_s}{2}$ and so eqn.92 reduces to:

$$\Psi_{\Sigma} \cong \frac{\gamma_M}{2\{1+\zeta^{-1}\}} \quad (95)$$

Transforming the latter expression into flux by noting that $\Psi_{\Sigma} = Lf_{\Sigma}/D_M\kappa_A a^{\infty}$ produces:

$$f_{\Sigma} \cong \frac{k_U\kappa_S s^{\infty} e_{\Sigma} L}{2\{1+\zeta^{-1}\}} = \frac{f_S}{2\{1+\zeta^{-1}\}} = \frac{k_U\kappa_S s^{\infty} e_{\Sigma} L}{2\left\{1+\frac{D_M/L}{k'}\right\}} \quad (96)$$

The result presented in eqn.96 is a modified version of case I previously discussed. This situation describes rate determining bimolecular reaction between substrate and oxidized enzyme (unsaturated enzyme kinetics) as outlined in eqn.43 and eqn.44. Note also that the rate of reaction between substrate and oxidized enzyme is much slower than that between reduced enzyme and oxidized mediator. Hence regeneration of oxidized enzyme is assumed to be rapid. Note that the observed flux f_{Σ} differs from that corresponding to the simple substrate flux, f_S via a term containing the loss factor $\zeta^{-1} = \frac{D_M/L}{k'} = \frac{D_M/L}{k^0} \exp[m\beta\xi]$ which depends on the ratio of mediator diffusion and mediator reaction at the underlying support electrode.

We now return to eqn.92 and consider the situation where substrate/enzyme reaction is much faster than substrate diffusion (again the regeneration of the oxidized enzyme is also assumed to be kinetically facile). This corresponds to the case where $\sqrt{\gamma_S} \gg 1$. Under these circumstances we can use the following approximation $\sec h\sqrt{\gamma_S} \cong 2\exp[-\sqrt{\gamma_S}]$ and $1 - \sec h\sqrt{\gamma_S} \cong 1 - 2\exp[-\sqrt{\gamma_S}] \cong 1$. Hence the general flux equation outlined in eqn.92 reduces to:

$$\Psi_{\Sigma} \cong \frac{\gamma_M/\gamma_S}{1+\zeta^{-1}} \quad (97)$$

Now we recall that the gamma parameter ratio is defined as $\gamma_M/\gamma_S = \frac{f_{SE}/f_{MD}}{f_{SE}/f_{SD}} = \frac{f_{SD}}{f_{MD}} = \frac{\kappa_S D_S s^{\infty}/L}{\kappa_A D_M a^{\infty}/L}$ and reflects therefore the diffusive rates of substrate and diffusion within the nanotube film. The flux expression presented in eqn.97 represents a new kinetic limiting case which we denote as case VII and label as the *titration* situation. Transforming to fluxes we obtain:

$$f_{\Sigma} \cong \frac{\kappa_S D_S s^{\infty}/L}{1+\frac{D_M/L}{k'}} \quad (98)$$

This kinetic situation pertains when diffusion of substrate through the nanotube layer is slow and rate determining. Again the magnitude of the flux observed at the underlying support electrode surface corresponding to reaction of the reduced mediator species is modified by the loss factor. In the

titration case the total flux is determined by the balance of fluxes of mediator and substrate to the reaction zone within the film.

Bartlett and Pratt [68] realized that under certain conditions in an enzyme modified electrode multilayer, the reaction kinetics may be mediator limited in one part of the film and substrate limited in another as a result of changes in substrate and mediator concentrations across the layer. This type of behaviour occurs when both mediator and substrate concentrations change significantly within the film. In a clever argument, Bartlett and Pratt [68] divided the enzyme layer into two regions (A and B, as illustrated in fig.2 of reference 68) divided by a demarcation line located at the critical distance $\chi = \varepsilon$. It was assumed that for $\chi < \varepsilon$ (region A) the kinetics were substrate limited and for $\chi > \varepsilon$ (region B) the kinetics were mediator limited. Bartlett and Pratt [68] solved approximate reaction diffusion equations appropriate to these two regions subject to the constraint that at the join between the two regions where $\chi = \varepsilon$ the concentrations and fluxes of substrate and mediator must match. It is possible using this approach after considerable algebraic analysis to obtain a useful expression for the observed reaction flux. Indeed this expression is presented in eqn.104. However life is too short for such long and convoluted analyses however erudite and consequently a more simple and direct approach to the final result will be developed.

This titration case mentioned in the previous paragraph can be developed using the following independent argument as also first noted by Bartlett and Pratt [68]. When the kinetics of the enzyme catalyzed reaction are fast the reaction occurs in a thin reaction zone somewhere within the nanotube film located at a distance $\chi = \varepsilon$. For $\chi > \varepsilon$ there is no reaction because $v \rightarrow 0$. For $\chi < \varepsilon$ there is no reaction because $u \rightarrow 0$. Now in the steady state the fluxes of substrate and mediator within the reaction zone must balance and so we can write that:

$$D_M \left(\frac{db}{dx} \right)_{x=\varepsilon} = -D_S \left(\frac{ds}{dx} \right)_{x=\varepsilon} \quad (99)$$

Or in normalized form:

$$\frac{D_M \kappa_A a^\infty}{L} \left(\frac{dv}{d\chi} \right)_{\chi=\varepsilon} = -\frac{\kappa_S D_S s^\infty}{L} \left(\frac{du}{d\chi} \right)_{\chi=\varepsilon} \quad (100)$$

The latter flux equality expression may be manipulated to produce

$$\left(\frac{dv}{d\chi} \right)_\varepsilon = -\frac{\gamma_M}{\gamma_S} \left(\frac{du}{d\chi} \right)_\varepsilon \quad (101)$$

Since the reaction occurs at $\chi = \varepsilon$ we can write that:

$$\begin{aligned} \left(\frac{dv}{d\chi} \right)_\varepsilon &= \frac{v_0}{\varepsilon} \\ \left(\frac{du}{d\chi} \right) &= \frac{1}{1-\varepsilon} \end{aligned} \quad (102)$$

Hence we can derive an expression for the critical distance ε by substituting eqn.102 into eqn.101 as follows: $(1-\varepsilon)v_0 = -(\gamma_M/\gamma_S)\varepsilon$. Further simplification produces:

$$\varepsilon = \frac{v_0}{v_0 - \frac{\gamma_M}{\gamma_S}} \quad (103)$$

Now the net flux is given by:

$$\Psi_\Sigma = -\frac{v_0}{\varepsilon} = \frac{\gamma_M}{\gamma_S} - v_0 \quad (104)$$

We recall that $v_0 = \zeta^{-1}\Psi_\Sigma$ and so eqn.104 reduces to:

$$\Psi_\Sigma = \left\{1 + \zeta^{-1}\right\} \frac{\gamma_M}{\gamma_S} \quad (105)$$

which was derived previously in eqn.97.

Bartlett and Pratt [68] have also noted that the result presented in eqn.104, derived for unsaturated Michaelis- Menten kinetic conditions, is quite general. The same expression also holds for $\alpha u \gg 1$. This is because in the substrate limited region of the film the substrate concentration is considerably less than its bulk value. Therefore the substrate concentration will be less than the Michaelis constant even though the bulk value may be greater.

Returning to the mediator reaction/diffusion master equation in the limit where $\alpha u \ll 1$ (eqn.87) we now examine the alternative limit corresponding to $\kappa u \gg 1$. Hence $\alpha \ll \kappa$. Under such circumstances eqn.87 reduces to:

$$\frac{d^2v}{d\chi^2} + \frac{\gamma_M}{\kappa} = 0 \quad (106)$$

This expression may be readily integrated twice to yield: $\frac{dv}{d\chi} = -\frac{\gamma_M}{\kappa}\chi + K_1$ and furthermore we obtain: $v = -(\gamma_M/2\kappa)\chi^2 + K_1\chi + K_2$. Noting that when $\chi=1$ $v=0$ implies $K_1 + K_2 = \gamma_M/2\kappa$ and also since $\chi=0$ $v=v_0 = \zeta^{-1}\Psi_\Sigma$ then $K_1 = \Psi_\Sigma = \left(\frac{dv}{d\chi}\right)_0$. Hence $\Psi_\Sigma \{1 + \zeta^{-1}\} = \gamma_M/2\kappa$. Simplifying we obtain:

$$\Psi_\Sigma = \frac{\gamma_M}{2\{1 + \zeta^{-1}\}\kappa} \quad (107)$$

The latter may be transformed into an expression for the observed flux:

$$f_\Sigma = \frac{\kappa_A k a^\infty e_\Sigma L}{2\{1 + \zeta^{-1}\}} = \frac{\kappa_A k a^\infty e_\Sigma L}{2\left\{1 + \frac{D_M/L}{k'}\right\}} \quad (108)$$

This is a modified form of case V corresponding to the situation of rate determining reaction between the oxidized mediator and reduced enzyme which occurs throughout the film. This reaction flux will be reduced by the diffusion of reduced mediator out of the layer given by the D_M/L term .

We now re-examine eqn.20, the master equation describing transport and kinetics of the redox mediator species and examine the limiting form when the substrate concentration is large when $\alpha u > 1$. Under these circumstances eqn.20 reduces to:

$$\frac{d^2v}{d\chi^2} + \frac{\gamma_M/\alpha}{1+\kappa/\alpha} = 0 \quad (109)$$

Again this expression may be readily integrated to yield: $\frac{dv}{d\chi} = -\frac{\gamma_M\alpha^{-1}}{1+\kappa\alpha^{-1}}\chi + K_1$ and $v = -\frac{\gamma_M\alpha^{-1}}{2\{1+\kappa\alpha^{-1}\}}\chi^2 + K_1\chi + K_2$. Again noting that $v=0$ $\chi=1$ implies that $K_1 + K_2 = \frac{\gamma_M\alpha^{-1}}{2\{1+\kappa\alpha^{-1}\}}$ and also noting that when $\chi=0$ $v=v_0 = \zeta^{-1}\Psi_\Sigma$ then $v_0 = K_2 = \zeta^{-1}\Psi_\Sigma$ and $\left(\frac{dv}{d\chi}\right)_0 = K_1 = \Psi_\Sigma$. Taking all these observations into consideration we obtain: $\Psi_\Sigma\{1+\zeta^{-1}\} = \gamma_M\alpha^{-1}/2\{1+\kappa\alpha^{-1}\}$. Consequently we obtain the following expression for the normalized flux under conditions of high substrate concentration:

$$\Psi_\Sigma = \frac{\gamma_M\alpha^{-1}}{2\{1+\zeta^{-1}\}(1+\kappa\alpha^{-1})} \quad (110)$$

If we examine the limit corresponding to $\kappa\alpha^{-1} \ll 1$ or $\kappa \ll \alpha$ then $1+\kappa\alpha^{-1} \cong 1$ and the normalized flux expression reduces to:

$$\Psi_\Sigma \cong \frac{\gamma_M}{2\alpha\{1+\zeta^{-1}\}} \quad (111)$$

Transforming the latter expression into flux by noting that $\Psi_\Sigma = Lf_\Sigma/D_M\kappa_A a^\infty$ produces:

$$f_\Sigma \cong \frac{k_c e_\Sigma L}{2\left\{1 + \frac{D_M/L}{k'}\right\}} \quad (112)$$

This is a modified form of case III. Hence when the substrate concentration is high ($\alpha \gg 1$) and when $\kappa\alpha^{-1} \ll 1$ or when κ is very small corresponding to $f_{SE} \ll f_{ME}$, the rate determining step corresponds to the situation where the enzyme-substrate adduct dissociates with a frequency defined by the catalytic rate constant k_c .

In contrast when $\kappa\alpha^{-1} \gg 1$ or $\kappa \gg \alpha$, eqn.110 reduces to: $\Psi_\Sigma \cong \frac{\gamma_M}{2\kappa\{1+\zeta^{-1}\}}$ which was outlined in eqn.108. Hence the flux is $f_\Sigma \cong \frac{\kappa_A k a^\infty e_\Sigma L}{2\left\{1 + \frac{D_M/L}{k'}\right\}}$ and we encounter a modified form of case

V again. Hence eqn.110 defines the connection between cases III and V. Hence under saturated conditions and when $f_{SE} \gg f_{ME}$ the mediator/enzyme reaction will be rate limiting.

2.7. The 'Magic' approximation

A key component in the reaction-diffusion expressions subjected to analysis in this paper is the non linear kinetic term presented in eqn.21 as $F(u) = \frac{u}{1 + \alpha u}$. In the analysis thus far we have simplified this term by taking the limit of $\alpha u \ll 1$ or $\alpha u \gg 1$ corresponding to unsaturated substrate kinetics or saturated substrate kinetics respectively. Ideally we would wish to develop an expression which would be valid for all values of the saturation parameter α . Both Bartlett [68] and Lyons [47] developed a useful expression sufficient for this purpose. Lyons [47] labeled this suggestion the 'Magic' approximation which states that :

$$\frac{u}{1 + \alpha u} \cong \frac{\alpha + u}{(1 + \alpha)^2} \quad (113)$$

We initially explore this approximation before using it to solve the reaction/diffusion expressions. Now if we set $\lambda = \alpha^{-1}$ then $u/(1 + \alpha u) = u/(1 + \lambda^{-1}u) = \lambda u/(\lambda + u) = \lambda \{u/(\lambda + u)\}$, and the approximation can be recast as:

$$\frac{u}{\lambda + u} \cong \frac{1 + \lambda u}{(1 + \lambda)^2} \quad (114)$$

It is immediately apparent that the approximation is exact when $u = 1$ for all values of λ . Hence the approximation is exact when substrate depletion in the modified electrode layer is negligible. As previously noted [47,68] the approximate expression becomes worse as u decreases or in other words as the degree of substrate depletion in the enzyme layer increases. It is least accurate for $u = 0$. For $\lambda \geq 1$ and $\lambda \gg u$:

$$\frac{u}{\lambda + u} \cong \frac{u}{\lambda} \cong \frac{1 + \lambda u}{\lambda^2} = \frac{\lambda^{-1} + u}{\lambda} \quad (115)$$

This expression will be valid for $u \gg \lambda^{-1}$. Under these conditions the function is approximately linear from 0 to λ^{-1} for u values from 0 to 1. In contrast when $\lambda \ll 1$ or $\lambda u \ll 1$ then

$$\frac{u}{\lambda + u} \cong 1 \quad (116)$$

and the expression is only valid for $u \gg \lambda$. Now the function is independent of u except for very low u values.

We now return to the master equations outlined in eqn.19 and eqn.20 and examine the limit at low κ . Hence

$$\frac{d^2u}{d\chi^2} - \frac{\gamma_s F(u)}{1 + \kappa F(u)} \cong \frac{d^2u}{d\chi^2} - \gamma_s F(u) = 0 \quad (117)$$

and

$$\frac{d^2v}{d\chi^2} + \frac{\gamma_m F(u)}{1 + \kappa F(u)} \cong \frac{d^2v}{d\chi^2} + \gamma_m F(u) = 0 \quad (118)$$

and we set

$$F(u) = \frac{u}{1+\alpha u} \cong \frac{\alpha+u}{(1+\alpha)^2} \quad (119)$$

to obtain the following expressions:

$$\frac{d^2u}{d\chi^2} - \frac{\gamma_s(\alpha+u)}{(1+\alpha)^2} = 0 \quad (120)$$

$$\frac{d^2v}{d\chi^2} + \frac{\gamma_M(\alpha+u)}{(1+\alpha)^2} = 0 \quad (121)$$

Turning attention to the u expression initially we can readily show that the solution to the differential equation is given by: $\frac{\gamma_s(\alpha+u)}{(1+\alpha)^2} = A \cosh\left[\frac{\sqrt{\gamma_s}\chi}{1+\alpha}\right] + B \sinh\left[\frac{\sqrt{\gamma_s}\chi}{1+\alpha}\right]$, which may be further simplified to obtain:

$$u = \frac{(1+\alpha)^2}{\gamma_s} \left\{ A \cosh\left[\frac{\sqrt{\gamma_s}\chi}{1+\alpha}\right] + B \sinh\left[\frac{\sqrt{\gamma_s}\chi}{1+\alpha}\right] \right\} - \alpha \quad (122)$$

Differentiating eqn.122 we obtain:

$$\frac{du}{d\chi} = \frac{(1+\alpha)}{\sqrt{\gamma_s}} \left\{ A \sinh\left[\frac{\sqrt{\gamma_s}\chi}{1+\alpha}\right] + B \cosh\left[\frac{\sqrt{\gamma_s}\chi}{1+\alpha}\right] \right\} \quad (123)$$

Now we note that when $\chi=0$ $\left(\frac{du}{d\chi}\right)_0 = 0$ and when $\chi=1$ $u=1$. Hence $B=0$ and also we

note that $A = \frac{\gamma_s}{1+\alpha} \operatorname{sech}\left[\frac{\sqrt{\gamma_s}}{1+\alpha}\right]$. We may immediately note that the normalized substrate flux is:

$$\Psi_s = \left(\frac{du}{d\chi}\right)_1 = \sqrt{\gamma_s} \operatorname{sech}\left[\frac{\sqrt{\gamma_s}}{1+\alpha}\right] \sinh\left[\frac{\sqrt{\gamma_s}}{1+\alpha}\right] = \sqrt{\gamma_s} \tanh\left[\frac{\sqrt{\gamma_s}}{1+\alpha}\right] \quad (124)$$

This expression is valid for all values of the saturation parameter α and connects the case I/case II regions over the entire range of α provided that $\kappa \ll 1$. Now for all values of α and for $\sqrt{\gamma_s} \ll 1$ when $f_{SE} \ll f_{SD}$ i.e. substrate diffusion through the layer is more rapid than substrate reaction then $\tanh\left[\frac{\sqrt{\gamma_s}}{1+\alpha}\right] \cong \frac{\sqrt{\gamma_s}}{1+\alpha}$ and the normalized flux reduces to:

$$\Psi_s \cong \frac{\gamma_s}{1+\alpha} \quad (125)$$

This expression is the appropriate form of eqn.36 derived in the thin layer approximation for the limiting circumstance of $\kappa \ll 1$. This expression transforms to the simple Michaelis-Menten equation describing rate determining reaction between the substrate and oxidized enzyme throughout the layer of thickness L :

$$f_s \cong \frac{k_c e_s L \kappa_s s^\infty}{K_M + \kappa_s s^\infty} \tag{126}$$

We can readily show that the substrate concentration profile valid for all values of saturation parameter is:

$$u = \operatorname{sech} \left[\frac{\sqrt{\gamma_s}}{1+\alpha} \right] \cosh \left[\frac{\sqrt{\gamma_s} \chi}{1+\alpha} \right] - \alpha \left\{ 1 - \operatorname{sech} \left[\frac{\sqrt{\gamma_s}}{1+\alpha} \right] \cosh \left[\frac{\sqrt{\gamma_s} \chi}{1+\alpha} \right] \right\} \tag{127}$$

This expression can be used to explore the solution to the mediator reaction-diffusion equation outlined in eqn.121 as follows. We note that $\alpha + u = (1+\alpha) \operatorname{sech} \left[\frac{\sqrt{\gamma_s}}{1+\alpha} \right] \cosh \left[\frac{\sqrt{\gamma_s} \chi}{1+\alpha} \right]$ and so the v equation reduces to

$$\frac{d^2 v}{d\chi^2} + \frac{\gamma_M}{1+\alpha} \operatorname{sech} \left[\frac{\sqrt{\gamma_s}}{1+\alpha} \right] \cosh \left[\frac{\sqrt{\gamma_s} \chi}{1+\alpha} \right] = 0 \tag{128}$$

This expression may be integrated to yield:

$$\begin{aligned} \frac{dv}{d\chi} &= -\frac{\gamma_M}{\sqrt{\gamma_s}} \operatorname{sech} \left[\frac{\sqrt{\gamma_s}}{1+\alpha} \right] \sinh \left[\frac{\sqrt{\gamma_s} \chi}{1+\alpha} \right] + K_1 \\ v &= -\frac{\gamma_M}{\gamma_s} (1+\alpha) \operatorname{sech} \left[\frac{\sqrt{\gamma_s}}{1+\alpha} \right] \cosh \left[\frac{\sqrt{\gamma_s} \chi}{1+\alpha} \right] + K_1 \chi + K_2 \end{aligned} \tag{129}$$

Since when $\chi=1$ $v=0$ we get $K_1 + K_2 = \frac{\gamma_M}{\gamma_s} (1+\alpha)$ and when $\chi=0$ $\left(\frac{dv}{d\chi} \right)_0 = \Psi_\Sigma = K_1$.

Hence we note that:

$$\Psi_\Sigma + K_2 = \frac{\gamma_M}{\gamma_s} (1+\alpha) \tag{130}$$

Furthermore since at $\chi=0$ $v=v_0 = \zeta^{-1} \Psi_\Sigma$, then $v_0 = \zeta^{-1} \Psi_\Sigma = -\frac{\gamma_M}{\gamma_s} (1+\alpha) \operatorname{sech} \left[\frac{\sqrt{\gamma_s}}{1+\alpha} \right] + K_2$

and so we finally obtain that $K_2 = \zeta^{-1} \Psi_\Sigma + \frac{\gamma_M}{\gamma_s} (1+\alpha) \operatorname{sech} \left[\frac{\sqrt{\gamma_s}}{1+\alpha} \right]$. When the latter is substituted into eqn.130 we obtain on simplification the following useful expression for the total normalized flux:

$$\Psi_\Sigma = \frac{\gamma_M (1+\alpha)}{\gamma_s \{1+\zeta^{-1}\}} \left\{ 1 - \operatorname{sech} \left[\frac{\sqrt{\gamma_s}}{1+\alpha} \right] \right\} \tag{131}$$

Again for $\sqrt{\gamma_s}/(1+\alpha) \ll 1$ we note that a suitable limiting expression for the observed reaction flux is:

$$\Psi_{\Sigma} \cong \frac{\gamma_M}{2\{1+\zeta^{-1}\}(1+\alpha)} \quad (132)$$

This is another modified form of case I (see eqn.96) valid for all saturation parameter values. This expression reduces to the following modified type of Michaelis-Menten rate equation:

$$f_{\Sigma} \cong \frac{k_c e_{\Sigma} L \kappa_S s^{\infty}}{2\left(1 + \frac{D_M/L}{k'}\right)(K_M + \kappa_S s^{\infty})} \quad (133)$$

This situation describes rate determining bimolecular reaction between substrate and oxidized enzyme for both unsaturated and saturated enzyme kinetics. Note also that the rate of reaction between substrate and oxidized enzyme is much slower than that between reduced enzyme and oxidized mediator. Hence regeneration of oxidized enzyme is assumed to be rapid. In contrast when $\sqrt{\gamma_S}/(1+\alpha) \gg 1$ the bracketed hyperbolic secant term in eqn.131 is effectively unity and the normalized flux reduces to:

$$\Psi_{\Sigma} \cong \frac{\gamma_M(1+\alpha)}{\gamma_S\{1+\zeta^{-1}\}} \quad (134)$$

This is a modified form of eqn.97 valid for all values of the saturation parameter and represents the titration case designated case VII. In terms of observed flux we obtain:

$$f_{\Sigma} \cong \frac{\kappa_S D_S s^{\infty}}{L} \left\{ \frac{1 + \frac{\kappa_S s^{\infty}}{K_M}}{1 + \frac{D_M/L}{k'}} \right\} \quad (135)$$

This kinetic situation pertains when diffusion of substrate through the nanotube layer is slow and rate determining. We note from eqn.135 that the diffusive flux of substrate through the layer is modified both by the substrate concentration and by the loss factor.

2.8. The kinetic case diagram

In this paper we have considered two distinct situations. The first refers to the conditions pertaining when the nanotube layer is conducting. The second refers to the situation when the nanotube layer is not so conducting. In doing so we have developed the pertinent reaction/diffusion equations for substrate and redox mediator, and obtained approximate analytical solutions for the latter non-linear differential equations which refer to various rate limiting situations. These limiting situations are defined in terms of the specific parameters κ , α and γ_S . Seven main kinetic limiting cases have been derived. Cases I-VI are identified for the conducting matrix problem, whereas for the not so conducting nanotube matrix four cases labeled I, III, V and VII are identified as stemming directly from the mathematical solution of the reaction-diffusion equations. These cases are outlined in table I

where expressions for the normalized flux and reaction flux are presented. In table II we present typical diagnostic criteria by which the correct case may be elucidated in an experimental situation. We indicate how the reaction flux or current depends (in effect the reaction order) with respect to changes in a particular experimental parameter such as substrate concentration, mediator concentration, enzyme loading or layer thickness. The latter may be readily varied experimentally. It is clear that each case presents a distinct quartet of reaction orders and so it is possible to identify a particular kinetically limiting case .

We summarize the theoretical results obtained in the paper in terms of a kinetic case diagram. These diagrams are presented in fig.7 and fig.8. In figure 7 the α, γ plane is outlined whereas in fig.8 the orthogonal α, κ plane is considered. In these figures we include the approximate limiting expressions for the normalized flux for each particular delineated kinetic case and also present the pertinent expressions connecting each of the limiting regions. The diagrams serve as a means by which the results of the detailed mathematical analysis may be conveniently represented in a very concise manner.

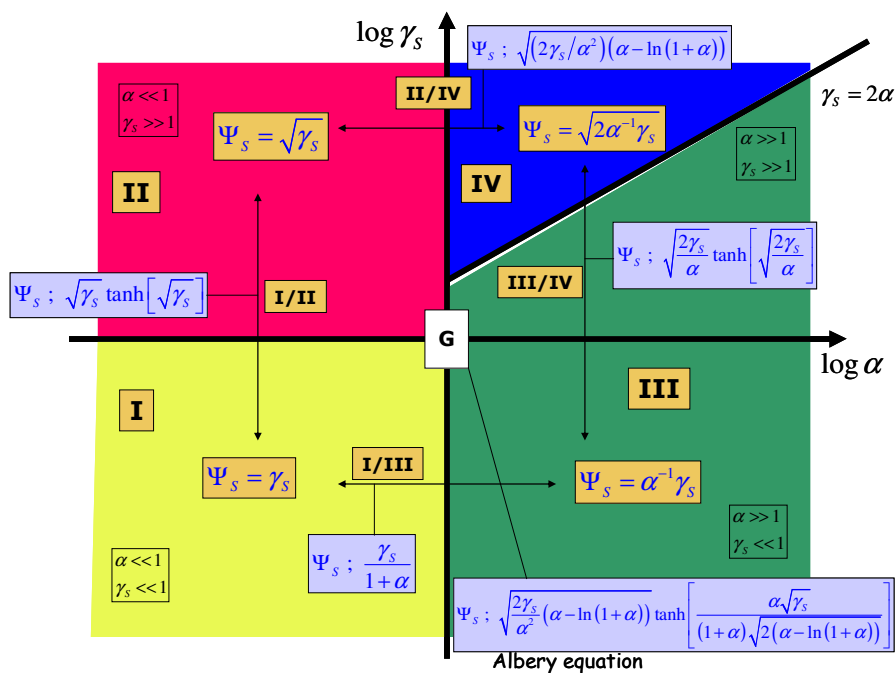


Figure 7. Kinetic case diagram illustrating the α, γ_s plane. The region designated G is the general case which is represented by the Albery equation.

Albery and co-workers [64] examined the kinetics of bound enzyme systems and suggested that the general expression for the substrate flux valid for the situation where γ_s and α are both close to unity (case G in figure 6) is given (using the present notation) by:

$$\Psi_s ; \sqrt{\frac{2\gamma_s}{\alpha^2}(\alpha - \ln(1 + \alpha))} \tanh \left[\frac{\alpha\sqrt{\gamma_s}}{(1 + \alpha)\sqrt{2(\alpha - \ln(1 + \alpha))}} \right] \tag{136}$$

Table 1. Typical expressions for reaction flux derived in text for approximate kinetic cases.

Kinetic Case	Normalised Flux	Reaction flux $f = i/nFA$
I	$\Psi_s = \gamma_s$ $\Psi_\Sigma = \frac{\gamma_M}{2\{1 + \zeta^{-1}\}}$	$f_s = \left(\frac{k_c}{K_M}\right) e_\Sigma L \kappa_s s^\infty$ $f_\Sigma = \frac{(k_c/K_M) \kappa_s s^\infty e_\Sigma L}{2\left\{1 + \frac{D_M/L}{k'}\right\}}$
II	$\Psi_s = \sqrt{\gamma_s}$	$f_s = \sqrt{\left(\frac{k_c}{K_M}\right) D_s e_\Sigma \kappa_s s^\infty}$
III	$\Psi_s = \frac{\gamma_s}{\alpha}$ $\Psi_\Sigma = \frac{\gamma_M}{2\{1 + \zeta^{-1}\} \alpha}$	$f_s = k_c e_\Sigma L$ $f_\Sigma = \frac{k_c e_\Sigma L}{2\left\{1 + \frac{D_M/L}{k'}\right\}}$
IV	$\Psi_s = \sqrt{2 \frac{\gamma_s}{\alpha}}$	$f_s = \sqrt{2 \kappa_s D_s k_c e_\Sigma s^\infty}$
V	$\Psi_s = \frac{\gamma_s}{\kappa}$ $\Psi_\Sigma = \frac{\gamma_M}{2\{1 + \zeta^{-1}\} \kappa}$	$f_s = k \kappa_A a^\infty e_\Sigma L$ $f_\Sigma = \frac{k \kappa_A a^\infty e_\Sigma L}{2\left\{1 + \frac{D_M/L}{k'}\right\}}$
VI	$\Psi_s = \sqrt{2 \frac{\gamma_s}{\kappa}}$	$f_s = \sqrt{2 \kappa_A k \kappa_s D_s e_\Sigma a^\infty s^\infty}$
VII	$\Psi_\Sigma = \frac{\gamma_M / \gamma_s}{1 + \zeta^{-1}}$	$f_\Sigma = \frac{\kappa_s D_s s^\infty / L}{1 + \frac{D_M/L}{k'}}$

Table 2. Typical diagnostic criteria for immobilized enzyme biosensors.

Case	s^∞	e_Σ	a^∞	L
I	1	1	0	1
II	1	1/2	0	0
III	0	1	0	1
IV	1/2	1/2	0	0
V	0	1	1	1
VI	1/2	1/2	1/2	1/2
VII	1	0	0	-1

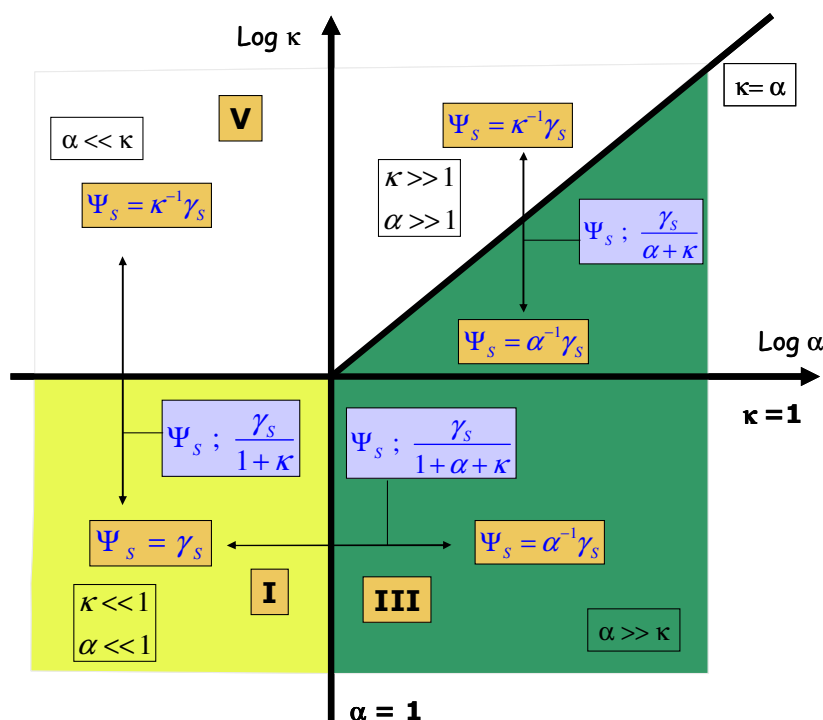


Figure 8. Kinetic case diagram illustrating the α, κ plane.

We indicate the shape of this expression in figure 7 and figure 8. In fig.7 the variation of normalized substrate flux with saturation parameter is presented for various values of the substrate reaction/diffusion parameter. These profiles typically exhibit the Michaelis-Menten biphasic kinetic behaviour [47]. It is interesting (see fig.7) that the normalized flux is predicted to decrease somewhat for larger values of α regardless of the value assumed for the substrate reaction diffusion parameter.

The expression outlined in eqn.136 has been applied also to describe amperometric detection in electroactive polymer thin films where Michaelis-Menten type adduct formation has been proposed to operate [47,68].. We now briefly consider the Bartlett-Pratt analysis [68] and see how it differs from the present approach.

The problem of reaction/diffusion of substrate and mediator within an electronically conducting polymer thin film containing immobilized enzyme molecules has been developed by Bartlett and Pratt [68]. This analysis has many elements in common with the current model and the reader is referred to the literature for full details of the analysis [68]. However to aid comparison between the present work and the Bartlett-Pratt model we provide in table 3 a direct comparison between the characteristic variables and parameters used in the present work and those alluded to in the Bartlett-Pratt paper.

Once this correspondence is taken into account the governing reaction diffusion equations developed by Bartlett and Pratt (see eqn.17 and eqn.18 of ref.[68]) can be seen to be equivalent to ours as presented in eqn.19 and eqn.20 of the present work.

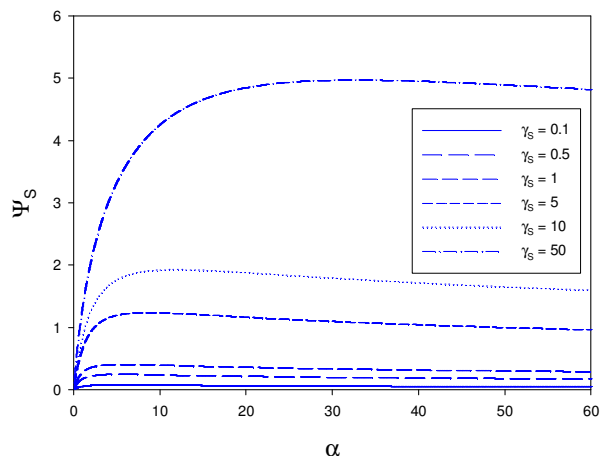


Figure 7. Plot of the Albery equation outlined in eqn.136 . The variation of normalized substrate flux with saturation parameter is outlined for various fixed values of the substrate reaction/diffusion parameter γ_S .

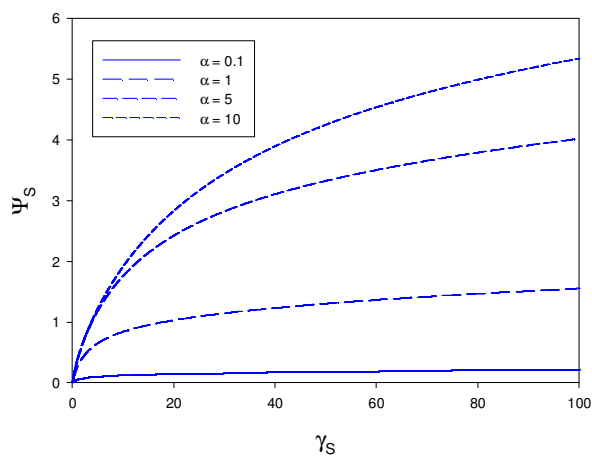


Figure 8. Plot of the Albery equation outlined in eqn.136 . The variation of normalized substrate flux with substrate reaction/diffusion parameter γ_S is outlined for various fixed values of the saturation parameter α .

Table 3. Direct comparison between Lyons and Bartlett-Pratt Models.

Present work	Bartlett-Pratt Model [68]
u	s
v	a
χ	χ
α	μ
K^{-1}	γ
λ_M	K^2
$K^{-1} \frac{\gamma_M}{\gamma_S}$	η

Bartlett and Pratt consider the case where the redox mediator is entrapped within the conducting polymer film (a case (i) scenario in the Bartlett-Pratt lexicon). This necessitates the use of slightly different boundary conditions at the film/solution interface corresponding to $\chi = 1$. In such a situation mediator entrapment implies that (in our notation), $\left(\frac{dv}{d\chi}\right)_1 = 0$. This will possibly correspond to the situation encountered for a redox hydrogel based biosensor. In contrast we have assumed that the oxidized form of the mediator is present in the bulk solution (corresponding to a case (ii) scenario in Bartlett-Pratt terminology). In contrast if the reduced form of the mediator is present in the bulk solution (such as is the situation when a substituted ferrocene species is used as redox mediator, labeled scenario (iii) by Bartlett and Pratt) and partitions into the film then the oxidized mediator concentration will be zero at the outer surface of the modified electrode and $1 - v_1 = 0$ or $v_1 = 1$ at $\chi = 1$. Bartlett and Pratt [68] also assumed that the relationship between the oxidized and reduced mediator concentration at the inner electrode/film interface is given by the Nernst equation. Instead we have proposed that mediator transformation at the underlying support electrode is given by the irreversible form of the Butler-Volmer equation.

We have considered seven distinct situations in the present paper. In all of these circumstances it is assumed that all the mediator and all the substrate diffusing into the film are consumed by the enzyme catalyzed reaction so that the concentration of substrate at the inner electrode surface and the concentration of reduced mediator at the outer film/solution interface are both zero. Bartlett and Pratt [68] have noted that this may not necessarily be the case. Two further cases may well exist in which either all the mediator or all the substrate is consumed within the film (see fig,3 in reference [68]). We do not consider these possibilities in the present paper.

3. CONCLUSIONS

In this paper we have presented a uniform model to describe substrate and redox mediator reaction kinetics and diffusion within a dispersed enzyme loaded carbon nanotube film of finite thickness. The pertinent reaction diffusion equations have been formulated, the pertinent boundary conditions appropriate to the situation where a redox mediator in its oxidized form is present in the solution adjacent to the enzyme film have been formulated, and approximate analytical expressions for the reaction flux obtained both for the situation when the film is conducting and when the film is less conducting. A series of distinct kinetic cases have been developed, and a prediction is made for the way in which the observed reaction flux (proportional to the steady state current) varies with changes in substrate and mediator concentration, with enzyme loading and with film thickness for each of these particular approximate cases. The mathematical analysis has been summarized in terms of kinetic case diagrams.

In the final paper in this trilogy we shall extend the theoretical analysis presented here to the more complex redox enzyme/metal nanoparticle/carbon nanotube systems.

ACKNOWLEDGEMENTS

This work was supported by Enterprise Ireland (grant number SC/2003/0049), IRCSET (Grant number SC/2002/0169) and the HEA-PRTL I Programme.

References

1. D. Chen, G. Wang, J. Li, *J. Phys. Chem.C.*, 111 (2007) 2351.
2. A.L. Ghindilis, P. Atanazov, E. Wilkins, *Electroanalysis*, 9 (1997) 661.
3. K. Habermuller, M. Mosbach, W. Schumann, *Fresenius J. Anal. Chem.*, 366 (2000) 366, 560.
4. W. Schumann, *Rev. Mol. Biotechnol.*, 82 (2002) 425.
5. S. Sek, R. Bilewicz, *J. Electroanal. Chem.*, 509 (2001) 11.
6. I. Willner, E. Katz, *Angew Chem. Int. Ed.*, 39 (2000) 1180.
7. A.N. Shipway, I. Willner, *Acc. Chem. Res.*, 34 (2001) 421.
8. E. Katz, I. Willner, *ChemPhysChem.*, 5 (2004) 1084.
9. J.J. Gooding, *Electrochim. Acta.*, 50 (2005) 3049.
10. Y.Lin, S. Taylor, H. Li, K.A. Shiral Fernando, L. Qu, W. Wang, L. Gu, B. Zhou, Y-P Sun, *J. Mater. Chem.*, 14 (2004) 527.
11. E. Katz, I. Willner, *Angew. Chem. Int. Ed.*, 43 (2004) 6042.
12. N.L. Rosi, C.A. Mirkin, *Chem. Rev.*, 105 (2005) 1547.
13. M. Keusgen, *Naturwissenschaften*, 89 (2002) 433.
14. J.C. Love, L.A. Estroff, J.K. Kriebel, R.G. Nuzzo, G.M. Whitesides, *Chem. Rev.*, 105 (2005) 1103.
15. M.E.G. Lyons, S. Rebouillat, *Int. Journal Electrochem. Sci.*, 4 (2009) 481.
16. S. Iijima, *Nature*, 354 (1991) 56.
17. K. Besteman, J.O. Lee, F.G.M. Wiertz, H.A. Heering, C. Dekker, *Nano Lett.*, 3 (2007) 727.
18. S.Rosenblatt, Y. Yaish, J. Park, J. Gore, V.Sazonova, P.L. McEuen, *Nano Lett.*, 2 (2002) 869.
19. I. Heller, A.M. Janssens, J. Mannik, D. Minot, S.G. Lemay, C. Dekker, *Nano Lett.*, 8 (2008) 591.
20. E. Bekyarova, M.E. Itkis, N. Cabrera, B. Zhao, A. Yu, J. Gao, R.C. Haddon, *J. Am. Chem. Soc.*, 127 (2005) 5990.
21. C.N.R. Rao, B.C. Satishkurnar, A. Govindaraj, M. Nath, *ChemPhysChem.*, 2 (2001) 78.
22. A.P. Graham, G.S. Duesberg, R.V. Seidel, M. Liebau, E. Unger, W. Pamler, F. Kreupl, W. Hoenlein, *Small*, 1 (2005) 382.
23. J. Wang, *Electroanalysis*, 17 (2005) 7.
24. R.R. Moore, C.E. Banks, R.G. Compton, *Anal. Chem.*, 76 (2004) 2677.
25. M.E.G. Lyons, G.P. Keeley, *Int.J. Electrochem. Sci.*, 3 (2008) 819.
26. L. Kavan, L. Dunsch, in *Carbon Nanotubes*, A.Jorio, G. Dresselhaus, M.S. Dresselhaus (Eds), *Topics Appl. Phys.*, , 111 (2008) 567-603.
27. X-J. Huang, H-S Im, O. Yarimaga, J-H Kim, D-Y Jang, D-H Lee, H-S Kim, Y-K Choi, *J. Electroanal. Chem.*, 594 (2006) 27.
28. J.Li, A. Cassell, L. Delzeit, J. Han, M. Meyyappan, *J. Phys. Chem. B.*, 106 (2002) 9299.
29. J.J. Gooding, R. Wibowo, J. Liu, W.Yang, D. Losic, S. Orbons, F.J. Mearns, J.G. Shapter, D.B. Hibbert, *J. Am. Chem. Soc.*, 125 (2003) 9006.
30. A. Chou, T. Bocking, N.K. Singh, J.J. Gooding, *Chem. Commun.*, 2005, 842.
31. G.G. Wildgoose, C.E. Banks, H.C. Leventis, R.G. Compton, *Microchim. Acta*, 152 (2006) 187.
32. J.M. Nugent, K.S.V. Santhanam, A. Rubio, P.M. Ajayan, *Nano Lett.*, 1 (2001) 87.
33. G.D. Withey, A.D. Lazareck, M.B. Tzolov, A. Yin, P. Aich, J.I. Yeh, J.M. Xu, *Biosens. & Bioelectron.*, 21 (2006) 1560.
34. P. Diao, Z. Liu, *J. Phys. Chem. B.*, 109 (2005) 20906.
35. H. Luo, Z. Shi, N. Li, Z. Gu, Q. Zhuang, *Anal. Chem.*, 73 (2001) 915.
36. C.E. Banks, R.R. Moore, T.J. Davies, R.G. Compton, *Chem. Commun.*, 2004, 1804.

37. J.M. Saveant, *Chem. Rev.*, 108 (2008) 2348.
38. C. Leger, *Chem. Rev.*, 108 (2008) 2379.
39. M.E.G. Lyons, *Electroactive Polymer Electrochemistry: Part 1: Fundamentals*, Plenum Press, New York, 1994 and references therein.
40. M.E.G. Lyons in *Polymeric Systems, Adv. Chem. Phys.* (I. Prigogine, S.A. Rice, Eds.) Wiley, New York, Vol. XCIV, 1996, pp.297-624.
41. A.R. Hillman, in *Electrochemical Science and Technology of Polymers*, R.G. Linford (ed) Elsevier, Amsterdam, 1987, pp.103-291.
42. G.P. Evans, in *Advances in Electrochemical Science and Engineering*, H. Gerisher, C.W. Tobias (eds.), VCH, Weinheim, vol.1, 1990, pp.1-74.
43. C.P. Andrieux, J.M. Saveant, in *Molecular Design of Electrode Surfaces, Techniques of Chemistry*, Vol.XXII, R.W. Murray (ed), Wiley Interscience, New York, 1992, pp.207-270.
44. M.E.G. Lyons, P.N. Bartlett, C.H. Lyons, W. Breen, J.F. Cassidy, J., *J. Electroanal. Chem.*, 304 (1991)1.
45. M.E.G. Lyons, C.H. Lyons, C.A. Fitzgerald, P.N. Bartlett, *J. Electroanal. Chem.*, 365 (1994) 29.
46. M.E.G. Lyons, *Analyst*, 119 (1994) 805.
47. M.E.G. Lyons, J.C. Greer, C.A. Fitzgerald, T. Bannon, P.N. Bartlett, *Analyst*, 121 (1996) 715.
48. L. Gorton, A. Torstensen, H. Jaegfeldt, G. Johansson *J. Electroanal. Chem.*, 161 (1984) 103
49. L. Gorton, G. Johansson, A. Torstensen, *J. Electroanal. Chem.*, 196 (1985) 81.
50. L. Gorton, *J. Chem. Soc., Faraday Trans I*, 86 (1986) 1245.
51. L.D. Burke, W.A. O'Leary, *J. Electrochem. Soc.*, 135 (1988) 1965.
52. M.E.G. Lyons, C.H. Lyons, D.E. McCormack, T. McCabe, W. Breen, J.F. Cassidy, *Anal. Proc.*, 28 (1991) 104.
53. M.E.G. Lyons, C.H. Lyons, A. Michas, P.N. Bartlett *J. Electroanal. Chem.*, 351(1993) 245.
54. W.J. Albery, A.R. Hillman, *J. Electroanal. Chem.*, 170 (1984) 27.
55. C.P. Andrieux, J.M. Dumas-Bouchiat, J.M. Saveant, *J. Electroanal. Chem.*, 87(1978)39.
56. C.P. Andrieux, J.M. Dumas-Bouchiat, J.M. Saveant, *J. Electroanal. Chem.*, 131(1982) 1
57. C.P. Andrieux, J.M. Dumas-Bouchiat, J.M. Saveant, *J. Electroanal. Chem.*, 169(1984) 9.
58. C.P. Andrieux, J.M. Saveant, *J. Electroanal. Chem.*, 171(1984)65.
59. M.E.G. Lyons, D.E. McCormack, A. Michas, P.N. Bartlett *Key Eng. Mater.*, 72 / 74 (1992) 477.
60. M.E.G. Lyons, C.H. Lyons, A. Michas, P.N. Bartlett (1992) *Analyst*, 117 (1992) 1271.
61. M.E.G. Lyons, T. Bannon, G. Hinds, S. Rebouillat, *Analyst*, 123(1998) 1947.
62. W.J. Albery, P.N. Bartlett, *J. Electroanal. Chem.*, 194 (1985) 211.
63. W.J. Albery, P.N. Bartlett, D.H. Craston, *J. Electroanal. Chem.*, 194(1985)223.
64. W.J. Albery, A.E.G. Cass, Z.X. Shu, *Biosens. & Bioelectron.*, 5 (1990) 367.
65. P.N. Bartlett, C.S. Toh, E.J. Calvo, V. Flexer, in *Bioelectrochemistry : Fundamentals, Experimental Reqniques and Applications*, Ed., P.N. Bartlett, Wiley, New York, 2008, Chapter 8, pp.267-326.
66. P.N. Bartlett, R.G. Whitaker, *J. Electroanal. Chem.*, 224 (1987) 27.
67. P.N. Bartlett, R.G. Whitaker, *J. Electroanal. Chem.*, 224 (1987) 37.
68. P.N. Bartlett, K.F.E. Pratt, *J. Electroanal. Chem.*, 397 (1995) 61.
69. P.N. Bartlett, P. Tebbutt, C.H. Tyrrell, *Anal. Chem.*, 64 (1992) 138.
70. P.N. Bartlett, K.F.E. Pratt, *Biosens. & Bioelectron.*, 8 (1993) 451.
71. M. Marchesiello, E. Genies, *J. Electroanal. Chem.*, 358 (1993) 35.
72. C. Bourdillon, C. Demaille, J. Moiroux, J.M. Saveant, *J. Am. Chem. Soc.*, 115 (1993) 2.
73. B. Limoges, J.M. Saveant, D. Yazidi, *J. Am. Chem. Soc.*, 125 (2003) 9192.
74. M. Dequaire, B. Limoges, J. Moiroux, J.M. Saveant, *J. Am. Chem. Soc.*, 124 (2002) 240.
75. N. Anicet, A. Anne, C. Bourdillon, C. Demaille, J. Moiroux, J.M. Saveant, *Faraday Discuss.*, 116 (2000) 269.
76. C. Bourdillon, C. Demaille, J. Moiroux, J.M. Saveant, *J. Phys. Chem., B*, 103 (1999) 8532.

77. C. Bourdillon, C. Demaille, J. Moiroux, J.M. Saveant, *Acc. Chem. Res.*, 29 (1996) 529.
78. M.E.G. Lyons, *Sensors*, 1 (2001) 215.
79. M.E.G. Lyons, *Sensors*, 2 (2002) 339.
80. M.E.G. Lyons, *Sensors*, 2 (2002) 473.
81. M.E.G. Lyons, *Sensors*, 3 (2003) 19.
82. M.E.G. Lyons, *Sensors*, 6 (2006) 1765.
83. R. Baronas, J. Kulys, *Sensors*, 8 (2008) 1.
84. J.J. Gooding, D.B. Hibbert, *Trends in Anal. Chem.*, 18 (1999) 525.
85. J.J. Gooding, L. Pugliano, D.B. Hibbert, P. Erokhin, *Electrochem. Commun.*, 2 (2000) 217.
86. J.J. Gooding, P. Erokhin, D. Losic, W. Yang, V. Policarpio, J. Liu, F.M. Ho, M. Situmorang, D.B. Hibbert, J.B. Shapter, *Anal. Sci.*, 17 (2001) 3.
87. J.J. Gooding, P. Erokhin, D.B. Hibbert, *Biosens. & Bioelect.*, 15 (2000) 229.
88. A.M. Kuznetsov, J. Ulstrup, *Electron transfer in chemistry and biology*, Wiley, New York, 1998 and references contained therein.
89. D.M. Adams et al. *J. Phys. Chem. B.*, 107 (2003) 6668.
90. A.M. Kuznetsov, J. Ulstrup, *J. Incl. Phenom. & Macrocycl. Chem.*, 35 (1999) 45.
91. I. Willner, B. Willner, E. Katz, *Rev. Mol. Biotech.*, 82 (2002) 325.
92. F.A. Armstrong, *Curr. Opin. Chem. Biol.*, 9 (2005) 110.
93. H.A. Heering, J. Hirst, F.A. Armstrong, *J. Phys. Chem. B.*, 102 (1998) 6889.
94. F.A. Armstrong, H.A. Heering, J. Hirst, *Chem. Soc. Rev.*, 26 (1997) 169.
95. C. Leger, S.J. Elliott, K.R. Hoke, L.J.C. Jeuken, A.K. Jones, F.A. Armstrong, *Biochem.*, 42 (2003) 8653.
96. M.J. Honeychurch, P.V. Bernhardt, *J. Phys. Chem. B.*, 108 (2004) 15900.
97. T. Reda, J. Hirst, *J. Phys. Chem. B.*, 110 (2006) 1394.
98. F.A. Armstrong, *Russ. J. Electrochem.*, 38 (2002) 49.
99. I. Willner, B. Willner, *Trends in Biotechnol.*, 19 (2001) 222.
100. I. Willner, E. Katz, *Angew. Chem. Int. Ed.*, 39 (2000) 1180.
101. K. Habermuller, M. Mosbach, W. Schuhmann, *Fresenius J. Anal. Chem.*, 366 (2000) 560.
102. W. Schuhmann, *Rev. Mol. Biotechnol.*, 82 (2002) 425.
103. A. Guiseppi-Elie, C. Lei, R.H. Baughman, *Nanotechnology*, 13 (2002) 559.
104. C. Cai, J. Chen, *Anal. Biochem.*, 332 (2004) 75.
105. W. Liang, Y. Zhuobin, *Sensors*, 3 (2003) 544.
106. M. Wang, Y. Shen, Y. Liu, T. Wang, F. Zhao, B. Liu, S. Dong, *J. Electroanal. Chem.*, 578 (2005) 121.
107. Y. Yin, Y. Lu, P. Wu, C. Cai, *Sensors*, 5 (2005) 220.
108. G. Wang, J.J. Hu, H.Y. Chen, *Electrochem. Commun.*, 4 (2002) 506.
109. J. Wang, M. Musameh, *Anal. Chem.*, 75 (2003) 2075.
110. M.E.G. Lyons, G.P. Keeley, *Chem. Commun.*, (2008) 2529.
111. J. Liu, A. Chou, W. Rahmat, M.N. Paddon-Row, J.J. Gooding, *Electroanalysis*, 17 (2005) 38.
112. M.E.G. Lyons, *Int. J. Electrochem. Sci.*, 4 (2009) 55.
113. M.E.G. Lyons, *Int. J. Electrochem. Sci.*, in preparation.
114. M.E.G. Lyons, D.E. McCormack, P.N. Bartlett, *J. Electroanal. Chem.*, 261 (1989) 51.
115. M.E.G. Lyons, P.N. Bartlett, *J. Electroanal. Chem.*, 316 (1991) 1.
116. M.E.G. Lyons, D.E. McCormack, O. Smyth, P.N. Bartlett, *Faraday Discuss. Chem. Soc.*, 88 (1989) 139.